

# Ligands with a 3,3-diphenylpentane skeleton for nuclear vitamin D and androgen receptors: Dual activities and metabolic activation

Shinnosuke Hosoda,<sup>a,\*</sup> Aya Tanatani,<sup>a</sup> Ken-ichi Wakabayashi,<sup>a</sup> Makoto Makishima,<sup>b</sup> Keisuke Imai,<sup>c</sup> Hiroyuki Miyachi,<sup>a</sup> Kazuo Nagasawa<sup>d</sup> and Yuichi Hashimoto<sup>a,\*</sup>

<sup>a</sup>*Institute of Molecular and Cellular Biosciences, The University of Tokyo, 1-1-1 Yayoi, Bunkyo-ku, Tokyo 113-0032, Japan*

<sup>b</sup>*Department of Biochemistry, Nihon University School of Medicine, 30-1 Oyaguchi-kamicho, Itabashi-ku, Tokyo 173-8610, Japan*

<sup>c</sup>*Drug Discovery Research, Astellas Pharma Inc., 21 Miyukigaoka, Tsukuba, Ibaraki 305-8585, Japan*

<sup>d</sup>*Department of Biotechnology and Life Science, Faculty of Technology, Tokyo University of Agriculture and Technology, 2-24-16 Naka-machi, Koganei-shi, Tokyo 184-8588, Japan*

Received 4 April 2006; revised 24 April 2006; accepted 25 April 2006

Available online 15 May 2006

**Abstract**—Ligands possessing dual vitamin D<sub>3</sub> (VD<sub>3</sub>)-agonistic and androgen-antagonistic activities with various activity spectra were prepared based on a substituted 3,3-diphenylpentane (DPP) skeleton. Among the compounds, (*R,S*)-DPP-1023 [(*R,S*)-7b] and (*S,S*)-DPP-0123 [(*S,S*)-7c] showed the most potent vitamin D<sub>3</sub>-agonistic activity [with potency comparable to that of 1 $\alpha$ ,25-dihydroxyvitamin D<sub>3</sub> (1,25-VD<sub>3</sub>)] and nuclear androgen receptor (AR)-binding activity (with higher affinity than that of hydroxyflutamide), respectively. Metabolic activation (reduction of the carbonyl group) of pivaloyl analogs [DPP-1113 (**3a**), DPP-1013 (**3b**), DPP-0113 (**3c**), and DPP-0013 (**3d**)] in HL-60 cells was found to be necessary for binding to nuclear vitamin D<sub>3</sub> receptor (VDR). © 2006 Elsevier Ltd. All rights reserved.

## 1. Introduction

Nuclear vitamin D receptor (VDR) is a member of the nuclear receptor superfamily and mediates various biological activities of its ligand, 1 $\alpha$ ,25-dihydroxyvitamin D<sub>3</sub> (1,25-VD<sub>3</sub>), which is a hormonally active form of vitamin D<sub>3</sub>.<sup>1–3</sup> The biological activities elicited by 1,25-VD<sub>3</sub> include regulation of calcium homeostasis, bone mineralization, proliferation and differentiation of various types of cells, and immune modulation.<sup>1–3</sup> Almost all of the important biological activities elicited by 1,25-VD<sub>3</sub> have been considered to be mediated by its binding to and activating VDR as a specific transcription factor.<sup>2,3</sup> More than 3000 derivatives with a secosteroidal skeleton have been designed and synthesized so far, and some of them have been shown to be full or partial bioisosters of 1,25-VD<sub>3</sub> (a full or partial bioisoster of 1,25-VD<sub>3</sub> is denoted as a VD-bioisoster in this paper).<sup>1</sup> Almost all of the known VD-bioisosters possess a secosteroidal skeleton.

However, Boehm et al. reported a novel structural type of VD-bioisosters, that is, compounds with a bis-phenol skeleton, including LG190178 (**7d**).<sup>4,5</sup> These compounds have been shown to be VD-bioisosters in a range of bioassay systems, including VDR reporter gene assay, monocytic cell differentiation-inducing activity toward human leukemia cell line HL-60, growth inhibition of human prostate tumor cell line LNCaP, regulation of VDR target gene expression in vivo, and so on.<sup>4</sup> Among these biological activities, HL-60 cell differentiation-inducing activity appeared to correlate well with the binding/activation of VDR by these compounds.<sup>1,6–8</sup> In fact, though only a few 1,25-VD<sub>3</sub> antagonists have been reported,<sup>9–12</sup> they were prepared based on VDR-binding assay and activity to repress 1,25-VD<sub>3</sub>-induced transcriptional activation in reporter gene assay, and they have been shown to possess inhibitory activity toward 1,25-VD<sub>3</sub>-induced HL-60 differentiation,<sup>9–12</sup> indicating that induction of HL-60 cell differentiation by 1,25-VD<sub>3</sub>- and at least some VD-bioisosters is mediated by binding to and activation of VDR.

We have been engaged in structural development studies of VD-bioisosters with a diphenylmethane skeleton derived from LG190178 (**7d**),<sup>4,5</sup> and have obtained several

**Keywords:** Vitamin D<sub>3</sub>; Androgen; Agonist; Antagonist; Metabolism; Diphenylpentane.

\* Corresponding authors. Tel.: +81 3 5841 7848; fax: +81 3 5841 8495 (S.H.); e-mail: [f46027@mail.ecc.u-tokyo.ac.jp](mailto:f46027@mail.ecc.u-tokyo.ac.jp)

VD-bioisosters with a nitrogen-containing 3,3-diphenylpentane (DPP) skeleton.<sup>13</sup> Although the correlation between VDR-binding and HL-60 differentiation-inducing activity of VD-bioisosters has been well-documented, our further investigation revealed that some of our VD-bioisosters with potent HL-60 cell differentiation-inducing activity lacked VDR-binding activity (vide infra).<sup>13</sup> We found that some of our VD-bioisosters also potently inhibit cell growth of androgen-dependent Shionogi carcinoma cell line SC-3.<sup>13</sup>

A relationship between VD-bioisosters and prostate cancer has been well documented.<sup>6,14–16</sup> For example, epidemiological evidence suggests that low exposure to sunlight and vitamin D deficiency may be risk factors for prostate cancer mortality.<sup>14,15</sup> In addition, 1,25-VD<sub>3</sub> and VD-bioisosters have been reported to induce apoptosis or differentiation in many cell types, including prostate tumor cell lines.<sup>6,16–18</sup> Although the VD-bioisoster-induced cell differentiation of HL-60 is mediated by direct binding and activation of VDR by the VD-bioisoster, the molecular mechanism and the role of VDR in VD-bioisoster-induced growth inhibition of androgen-dependent cell lines remain obscure.<sup>6–8</sup> Our recently reported preliminary studies<sup>13</sup> led us suspect that some VD-bioisosters might act as antagonists of androgen at the nuclear androgen receptor (AR)-binding level.

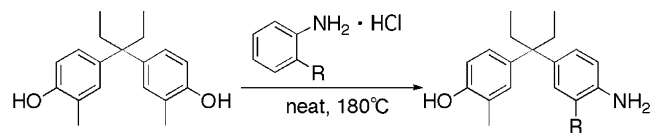
Therefore, we started a detailed investigation of VD-bioisosters with a 3,3-diphenylpentane (DPP) skeleton. In this paper, we describe the preparation of the VD-bioisosters (**3a–d** and **7a–c**), evaluation of their biological activities, that is, vitamin D<sub>3</sub> activity measured as HL-60 cell differentiation-inducing activity, VDR-binding activity, nuclear androgen receptor (AR)-binding activity, and androgen-antagonistic activity measured as growth inhibition of SC-3 cells. The great difference between vitamin D<sub>3</sub> activity at the HL-60 cell level and VDR-binding activity found in some VD-bioisosters could be explained in terms of participation of metabolic activation of the corresponding VD-bioisosters in the cells.

## 2. Chemistry

Based on our previous study,<sup>13</sup> we focused on aza-analogs of LG190178 (**7d**),<sup>4,5</sup> that is, compounds **7a–c** and their pivaloyl derivatives, **3a–d**. Some of these compounds, though they were diastereomeric mixtures, have been shown to elicit dual vitamin D<sub>3</sub>-agonistic (estimated as HL-60 monocytic cell differentiation induction) and androgen-antagonistic (estimated as testosterone-induced SC-3 cell growth inhibition) activities with various activity spectra.<sup>13</sup>

3,3-Bis(4-amino-3-methylphenyl)pentane (DPP-1100: **1**) and 4-[3-(4-amino-3-methylphenyl)pentane-3-yl]-2-methylphenol (DPP-0100: **4**) were prepared as described previously.<sup>13</sup> Briefly, Buchwald–Hartwig's amination reaction<sup>19,20</sup> of 3,3-bis[4-(trifluoromethylsulfonyl)-3-methylphenyl]pentane gave DPP-1100 (**1**). DPP-0100 (**4**) was prepared by direct substitution of 3,3-bis

**Table 1.** Substitution reaction of bis-phenol with substituted aniline



R	Reaction times (h)	Yield (%)
H	5	57
Me	4	65
<i>i</i> -Pr	15	72
Bn	12	62

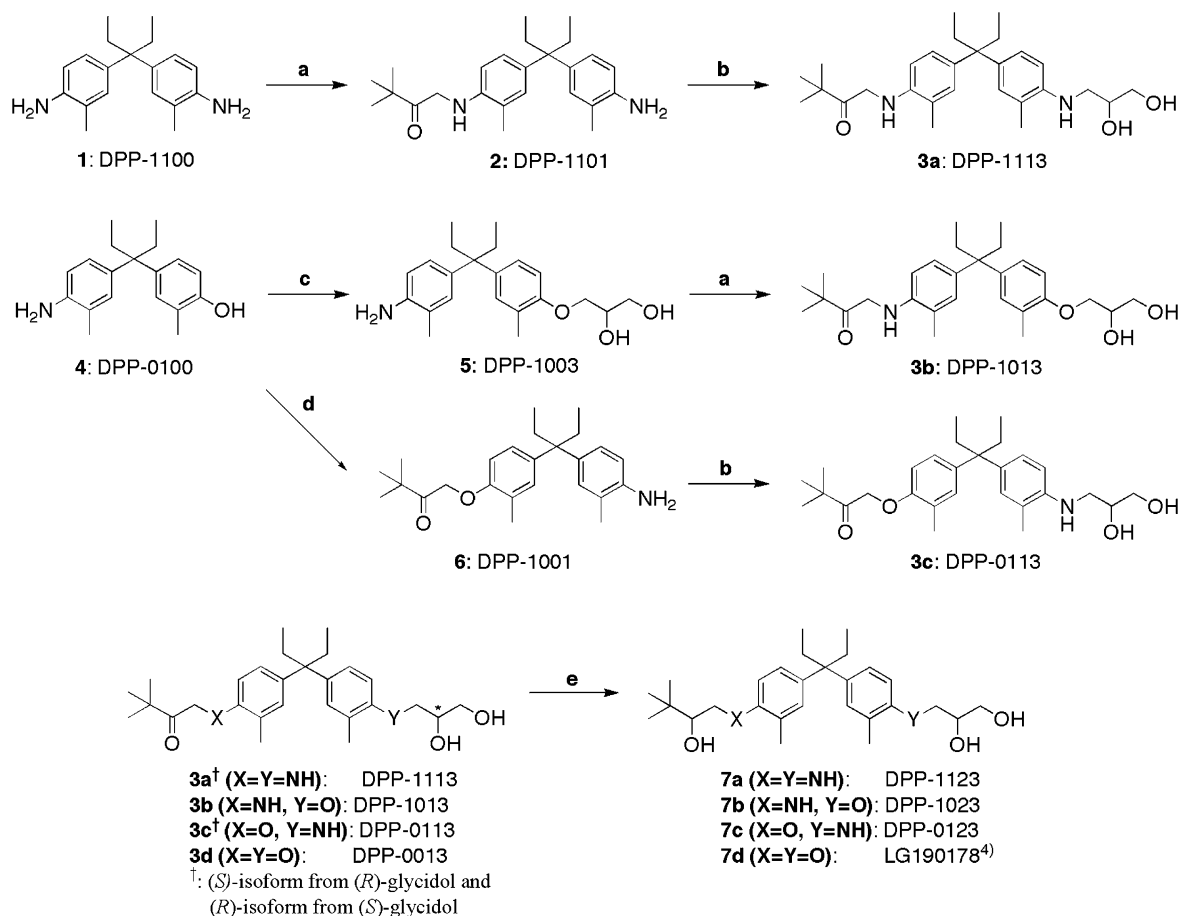
(4-hydroxy-3-methylphenyl)pentane with *ortho*-toluidine hydrochloride (neat, 180 °C, 2.5 h) in the yield of 65%.<sup>13,21</sup> This substitution gave only the mono-substituted product even in the presence of an excess amount of *ortho*-toluidine hydrochloride. Other substituted analogs of DPP-0100 (**4**) could be obtained by similar reaction in moderate to good yield (Table 1). Each hydroxyl group and amino group was alkylated to give compounds **3a–d**, followed by reduction of a carbonyl group to give compounds **7a–d** as shown in Scheme 1. Compound **7d** (LG190178) has already been reported, though as a diastereomeric mixture.<sup>4</sup>

By the use of optically pure isoforms of glycidol in reactions b and c in Scheme 1, optically pure isoforms of **3a–d** could be obtained. Reduction of a carbonyl group of the pivaloyl moiety of compounds **3a–d** with NaBH<sub>4</sub> gave epimeric mixtures of triols (**7a–d**), which were separated by chiral HPLC to give pure optical isomers. The configuration of the secondary alcohol created by the reduction was determined by the modified Mosher's method [a (+)- or (–)- $\alpha$ -methoxy- $\alpha$ -(trifluoromethyl)phenylacetyl (MTPA) group was introduced at the secondary alcohol group after protecting the diol moiety as dimethylacetal].<sup>22</sup>

In this paper, all the structures are drawn so as to put the pivaloyl or its reduced form (if present) on the left side, and vicinal diol moiety (if present) on the right side. The code names of the compounds used in this paper are in the form DPP followed by four numbers; application of this nomenclature is illustrated in Figure 1. DPP stands for the 3,3-diphenylpropane skeleton. The first number represents the heteroatom on the left side, and the second represents that on the right side: oxygen (0) or nitrogen (1). The third number represents the substituent on the left heteroatom, and the fourth represents that on the right heteroatom: no side chain (0), a pivaloyl group (1), a reduced pivaloyl substituent (2), and a vicinal diol group (3). For compounds **7a–d**, the configurations (*S* or *R*) of the left- and right-side chains are represented by the first and the second letters, respectively, in parentheses before the code name.

## 3. Vitamin D<sub>3</sub>-agonistic activity

The relative binding affinities of the compounds to VDR and the vitamin D<sub>3</sub>-agonistic activity measured



**Scheme 1.** Preparation of compounds **3a–d** and **7a–d**. Reagents and conditions: (a) 1-chloropinacolone, Et<sub>3</sub>N, KI, DMF, rt, 38–48%; (b) glycidol, EtOH, 85 °C, 26–69%; (c) glycidol, CsF, DMF, 85 °C, 71%; (d) NaH, 1-chloropinacolone, DMF, rt, 97%; (e) NaBH<sub>4</sub>, MeOH, rt, 89–99%.

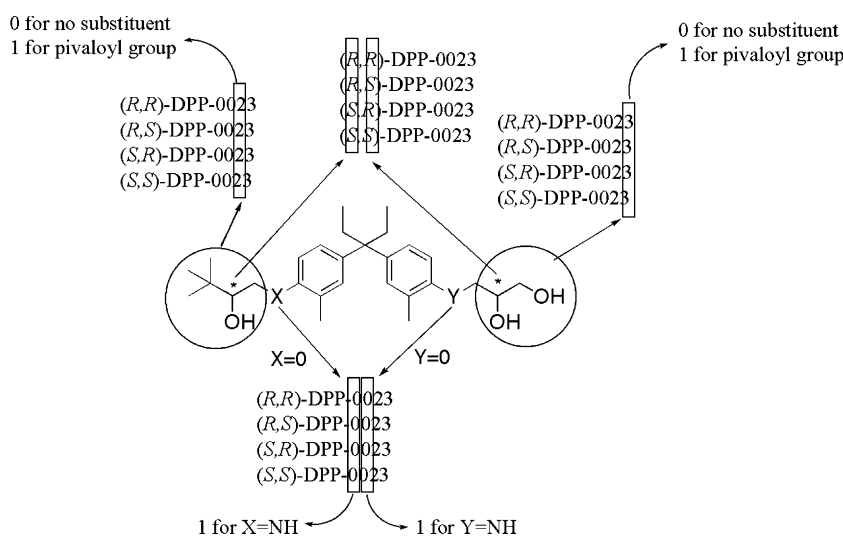


**Figure 1.** Basis of the code names of the compounds (see text).

as HL-60 cell differentiation-inducing activity were examined using the method described previously (see Section 7).<sup>11,12,23–25</sup> Of course, values of the relative binding affinities of test compounds to VDR and those of the cell differentiation-inducing activity differed from experiment to experiment, but the results

were basically reproducible. A typical set of data is presented in Table 2.

For the first screening of the compounds, we used enantiomeric and diastereomeric mixtures of **3a–d** and **7a–d**, respectively (entries 2–6, 11, 16, and 21 in Table 2). As

**Table 2.** Vitamin D<sub>3</sub>-agonistic activity of 3,3-diphenylpentane derivatives

Entry	Compound	VDR affinity (K <sub>i</sub> , nM)	HL-60 differentiation induction (EC <sub>50</sub> , nM)
1	1,25-VD <sub>3</sub>	0.17	9
2	DPP-1113 ( <b>3a</b> ) <sup>a</sup>	>5000	850
3	DPP-1013 ( <b>3b</b> ) <sup>a</sup>	3600	360
4	DPP-0113 ( <b>3c</b> ) <sup>a</sup>	>5000	110
5	DPP-0013 ( <b>3d</b> ) <sup>a</sup>	>5000	90
6	DPP-1123 ( <b>7a</b> ) <sup>b</sup>	260	37
7	( <i>R,R</i> )-DPP-1123 [( <i>R,R</i> )- <b>7a</b> ]	190	48
8	( <i>S,R</i> )-DPP-1123 [( <i>S,R</i> )- <b>7a</b> ]	580	170
9	( <i>R,S</i> )-DPP-1123 [( <i>R,S</i> )- <b>7a</b> ]	120	6.6
10	( <i>S,S</i> )-DPP-1123 [( <i>S,S</i> )- <b>7a</b> ]	350	43
11	DPP-1023 ( <b>7b</b> ) <sup>b</sup>	52	48
12	( <i>R,R</i> )-DPP-1023 [( <i>R,R</i> )- <b>7b</b> ]	150	30
13	( <i>S,R</i> )-DPP-1023 [( <i>S,R</i> )- <b>7b</b> ]	180	55
14	( <i>R,S</i> )-DPP-1023 [( <i>R,S</i> )- <b>7b</b> ]	9.5	4.1
15	( <i>S,S</i> )-DPP-1023 [( <i>S,S</i> )- <b>7b</b> ]	20	16
16	DPP-0123 ( <b>7c</b> ) <sup>b</sup>	930	52
17	( <i>R,R</i> )-DPP-0123 [( <i>R,R</i> )- <b>7c</b> ]	340	320
18	( <i>S,R</i> )-DPP-0123 [( <i>S,R</i> )- <b>7c</b> ]	1100	770
19	( <i>R,S</i> )-DPP-0123 [( <i>R,S</i> )- <b>7c</b> ]	220	47
20	( <i>S,S</i> )-DPP-0123 [( <i>S,S</i> )- <b>7c</b> ]	420	110
21	LG190178 ( <b>7d</b> ) <sup>b,4</sup>	360	44
22	( <i>R,R</i> )-LG190178 [( <i>R,R</i> )- <b>7d</b> ]	320	26
23	( <i>S,R</i> )-LG190178 [( <i>S,R</i> )- <b>7d</b> ]	740	120
24	( <i>R,S</i> )-LG190178 [( <i>R,S</i> )- <b>7d</b> ]	12	8.6
25	( <i>S,S</i> )-LG190178 [( <i>S,S</i> )- <b>7d</b> ]	11	23

<sup>a</sup> Enantiomeric mixture.<sup>b</sup> Diastereomeric mixture.

shown in the table, pivaloyl derivatives **3a–d** (entries 2–5) possessed no or very weak VDR-binding activity. However, in spite of their lack of affinity for VDR, they showed moderate to rather potent HL-60 cell differentiation-inducing activity. DPP-0113 (**3c**) and DPP-0013 (**3d**) showed rather potent differentiation-inducing activity with EC<sub>50</sub> values of 90–110 nM, even though they did not bind to VDR (vide infra). On the other hand, reduction of the carbonyl group at the pivaloyl moiety of **3a–d** to an alcoholic group, that is, **7a–d** (entries 6, 11, 16, and 21), resulted in appearance of VDR-binding activity (*K<sub>i</sub>* values of 52–930 nM) and enhancement of HL-60 cell differentiation-inducing activity (EC<sub>50</sub> values of 37–52 nM). Exchange of one or two phenolic oxygens of LG190178 (**7d**) for nitrogen seemed to not affect the HL-60 cell differentiation-inducing activity (compare entry 21 with entries 6, 11, and 16), but seemed to enhance [for DPP-1123 (**7a**) and DPP-1023 (**7b**)] or decrease [for DPP-0123 (**7c**)] the affinity for VDR.

On the basis of this first screening result, we evaluated optically pure isomers of **7a–d** (entries 7–10, 12–15, 17–20, and 22–25 in Table 2). There seemed to be a reasonably good correlation between affinity for VDR and HL-60 cell differentiation-inducing activity for all optical isomers of **7a–d**. For DPP-1123 (**7a**: entries 7–10),

DPP-1023 (**7b**: entries 12–15), and DPP-0123 (**7c**: entries 17–20), the (*R,S*)-isomers (entries 9, 14, and 19) showed the most potent activities among the series, as regards both affinity for VDR and HL-60 cell differentiation induction. (*R,S*)-LG190178 [(*R,S*)-**7d**] showed the most potent HL-60 cell differentiation-inducing activity among the optical isomers (entries 22–25), though its VDR-binding activity was comparable to that of (*S,S*)-LG190178 [(*S,S*)-**7d**]. In HL-60 cell differentiation-inducing assay, the (*R,S*)-isomers were the most potent 1,25-VD<sub>3</sub> agonists among the optical isomers in each series, and the enantiomers, that is, the (*S,R*)-isomers, showed the lowest activities in both VDR-binding and HL-60 cell differentiation-inducing assays (entries 8, 13, 18, and 23). (*R,S*)-DPP-1023 [(*R,S*)-**7b**] showed the most potent activity among the (*R,S*)-isomers for both VDR-binding and HL-60 cell differentiation, with the latter activity being more potent (EC<sub>50</sub> = 4.1 nM: entry 14) than that of 1,25-VD<sub>3</sub> (EC<sub>50</sub> = 9 nM: entry 1).

#### 4. Metabolic activation of pivaloyl analogs to elicit vitamin D<sub>3</sub> activity

As mentioned above, one of our nitrogen-containing pivaloyl analogs, DPP-0113 (**3c**), showed rather potent differentiation-inducing activity, though it did not bind VDR (entry 4 in Table 2). DPP-0113 (**3c**) did not bind to or activate other HL-60 differentiation-related nuclear receptors, including retinoic acid receptors (RARα, β, and γ) and retinoid X receptors (RXRα, β, and γ), or VDR extracted from HL-60 cells (data not shown). However, the HL-60 cell differentiation-inducing activity of DPP-0113 (**3c**) was apparently inhibited by a competitive vitamin D<sub>3</sub> antagonist with a secosteroidal skeleton, (23*S*,25*S*)-DLAM-1P (Fig. 2).<sup>11,12</sup> This result suggested that the HL-60 cell differentiation induced by DPP-0113 (**3c**) is mediated by the VDR pathway, at least in part. Therefore, we suspected that DPP-0113 (**3c**) might be metabolized in HL-60 cells to a derivative(s) which possesses affinity for VDR. In fact, treatment of DPP-0113 (**3c**) with a homogenate prepared

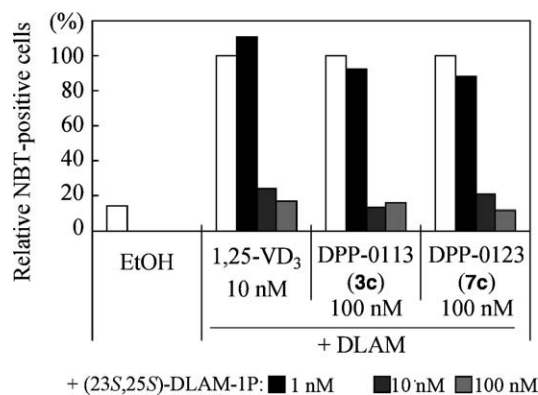


**Figure 2.** Inhibitory effect of (23*S*,25*S*)-DLAM-1P<sup>11,12</sup> on HL-60 cell differentiation induced by 1,25-VD<sub>3</sub>, DPP-0113 (**3c**) and DPP-0123 (**7c**). Vertical scale: relative population of NBT-positive cells (%). The percentage of NBT-positive cells in the incubation mixture treated with 10 nM 1,25-VD<sub>3</sub> alone was defined as 100%.

from HL-60 cells resulted in the appearance of VDR-binding activity (Fig. 3), suggesting metabolic activation of the compound to a VDR ligand(s). In contrast, the same treatment of DPP-0123 (**7c**), which possesses moderate VDR-binding affinity (entry 16 in Table 2), did not affect its VDR-binding activity (Fig. 3).

To examine the metabolism of DPP-0113 (**3c**), we used optically pure (*S*)-DPP-0113 [(*S*)-**3c**] and (*R*)-DPP-0113 [(*R*)-**3c**], because metabolism of these compounds would create another asymmetric center(s). (*S*)-DPP-0113 [(*S*)-**3c**] and (*R*)-DPP-0113 [(*R*)-**3c**] were treated with homogenate prepared from HL-60 cells, and then analyzed by means of HPLC with a chiral column (Fig. 4). As shown in Fig. 4, for both (*S*)-DPP-0113 [(*S*)-**3c**] and (*R*)-DPP-0113 [(*R*)-**3c**], only two major peaks of metabolites were detected. These peaks were identified as the analogs in which the carbonyl group of the pivaloyl moiety is reduced to an alcoholic group, by means of HPLC and mass spectroscopic analysis. Treatment with HL-60 cell homogenate of (*S*)-DPP-0113 [(*S*)-**3c**] and (*R*)-DPP-0113 [(*R*)-**3c**] resulted in the appearance of (*R,S*)- and (*S,S*)-DPP-0123 [(*R,S*)- and (*S,S*)-**7c**] and (*R,R*)- and (*S,R*)-DPP-0123 [(*R,R*)- and (*S,R*)-**7c**], respectively, which are triol derivatives (**7c**) possessing VDR-binding affinity (entries 17–20 in Table 2).

These results suggested that pivaloyl derivatives (**3a–d**) are metabolically reduced to the corresponding VDR-binding **7a–d** in HL-60 cells. In other words, the pivaloyl derivatives (**3a–d**) might be intrinsically inactive pro-drugs, which elicit vitamin D<sub>3</sub>-agonistic activity mediated by VDR only upon metabolic reduction. To examine the role of the additional hydroxyl group in **7a–d**, we performed a preliminary computer-assisted docking study of (*R,S*)-DPP-0123 [(*R,S*)-**7c**] with VDR (Fig. 5), based on the VDR–LBD (recombinant-ligand binding domain of VDR) X-ray structure of the VDR–LBD/1,25-VD<sub>3</sub> complex.<sup>26</sup>

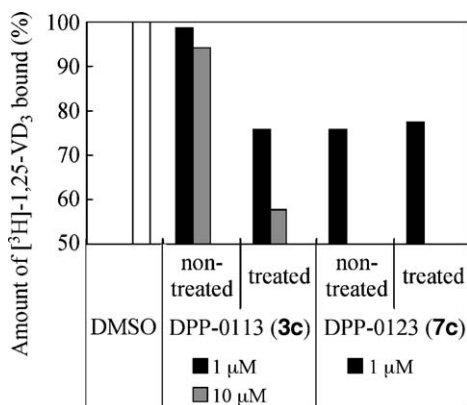


**Figure 3.** Effect of treatment of DPP-0113 (**3c**) and DPP-0123 (**7c**) with HL-60 cell homogenate on binding activity toward VDR [<sup>3</sup>H]-1,25-VD<sub>3</sub> was added at 1 nM concentration. Non-treated: DPP-0113 (**3c**) or DPP-0123 (**7c**) was added directly to determine the VDR-binding competition activity. Treated: DPP-0113 (**3c**) or DPP-0123 (**7c**) was added after incubation with HL-60 cell homogenate.

First, computer-assisted reconstruction studies of the VDR–LBD/1,25-VD<sub>3</sub> complex were performed to test the reliability of the docking calculation. Namely, 1,25-VD<sub>3</sub> was deleted from the reported X-ray structure of VDR–LBD/1,25-VD<sub>3</sub> complex (PDB:1DB1) and the remaining VDR–LBD structure was used as a rigid receptor model. Energy minimization of the complex structure with VDR–LBD and 1,25-VD<sub>3</sub> was performed with the CHARMM<sup>®</sup> force field<sup>27</sup> until a gradient convergence of less than 0.01 kcal/mol Å was reached. The obtained docking structure was consistent with the X-ray structure, supporting the reliability of our calculation method.

Then, (*R,S*)-DPP-0123 [(*R,S*)-**7c**] was docked under the same conditions and gave a similar docking structure to that of 1,25-VD<sub>3</sub> (Fig. 5). As shown in Fig. 5, the metabolically generated hydroxyl group of (*R,S*)-DPP-0123 [(*R,S*)-**7c**] interacts with His 397 of VDR–LBD through hydrogen-bonding, as the 25-hydroxyl group of 1,25-VD<sub>3</sub> does. This interaction is known to be one of the critical factors for ligand binding to VDR. The vicinal diol moiety of (*R,S*)-DPP-0123 [(*R,S*)-**7c**] interacts with Tyr 143 and Ser 237 through hydrogen-bonding, as do the 1 $\alpha$ - and 3 $\beta$ -hydroxyl groups of 1,25-VD<sub>3</sub>, respectively.

## 5. Androgen-antagonistic activity

Previously, we reported that some DPP-analogs, including a pivaloyl derivative DPP-0113 (**3c**, enantiomeric mixture, entry 7 in Table 3), possess androgen-antagonistic activity, as evaluated in terms of inhibitory activity on testosterone-induced cell growth of the androgen-dependent cell line SC-3.<sup>13,28–31</sup> Our preliminary studies suggested that DPP-0113 possesses AR-binding activity.<sup>13</sup> So, we prepared optically pure isomers of **3a–d**, and evaluated their AR-binding activity using recombinant human AR protein, as previously reported (Table 3, see Section 7). In contrast to the case of VDR-binding activity, all the pivaloyl analogs showed moderate to potent AR-binding activity with *K<sub>i</sub>* values of 720–7400 nM (entries 3–6 and 8–11 in Table 3), suggesting that metabolic activation (reduction of the pivaloyl group) is not necessary to elicit AR-binding activity. Among the compounds, (*S*)-DPP-0113 [(*S*)-**3c**, entry 9] showed the most potent AR-binding activity (*K<sub>i</sub>* = 720 nM); this compound is more potent than hydroxyflutamide (*K<sub>i</sub>* = 940 nM, entry 2), an active form of the clinically useful anti-androgenic drug, flutamide.

The AR-binding activities of the triol derivatives (**7a–d**) in their optically pure forms were also evaluated (entries 12–27 in Table 3). For DPP-1123 (**7a**: entries 12–15), DPP-1023 (**7b**: entries 16–19), and DPP-0123 (**7c**: entries 20–23), the (*S,S*)-isomers (entries 15, 19, and 23) showed the most potent AR-binding activity in each series of compounds, in contrast to the case of vitamin D<sub>3</sub>-agonistic activity, where the (*R,S*)-isomers are the eutomers. (*S,S*)-DPP-0123 [(*S,S*)-**7c**] showed the most potent activity, with a *K<sub>i</sub>* value of 400 nM (entry 23). Nevertheless,

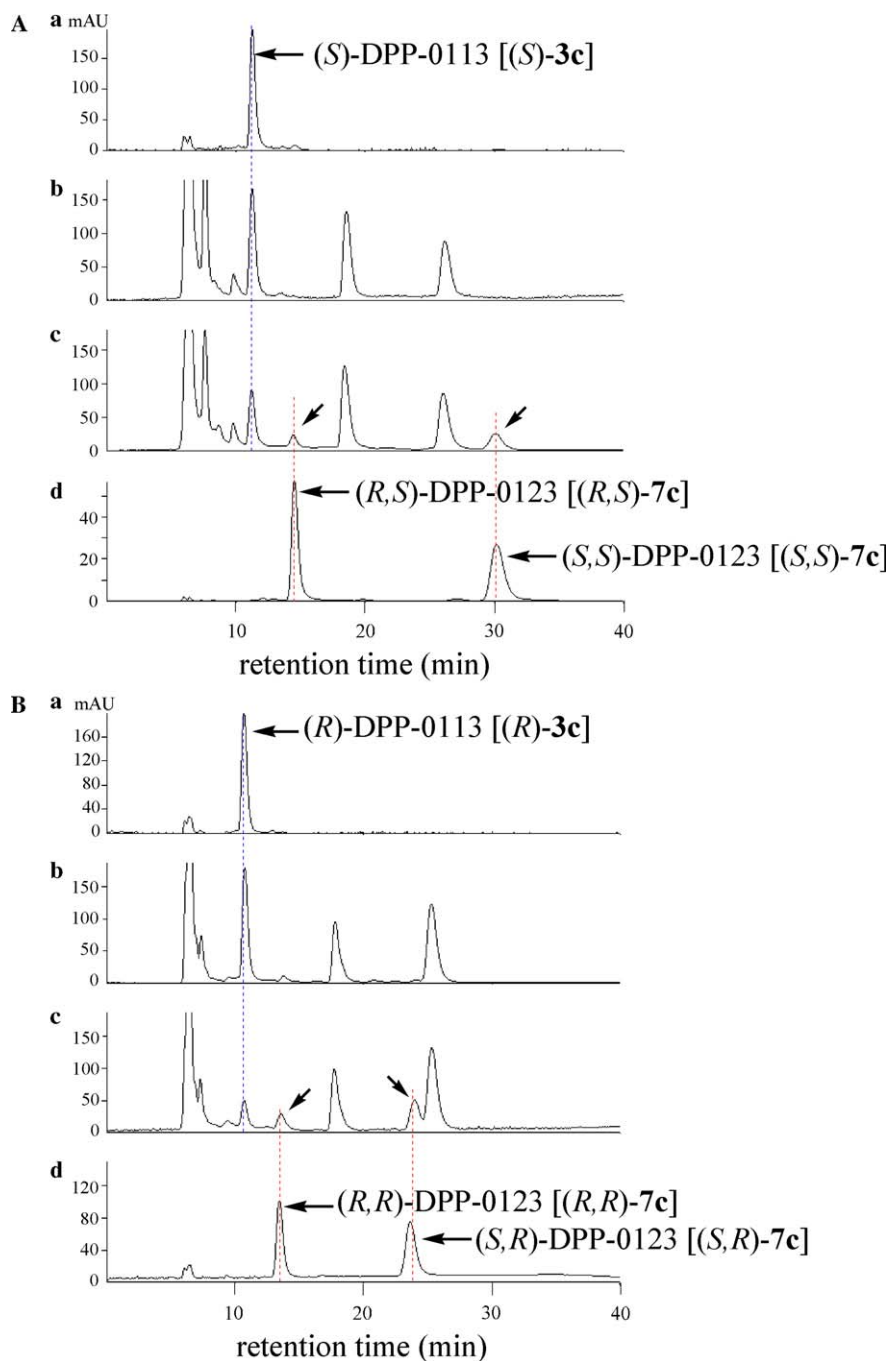


**Figure 4.** HPLC analysis of metabolites of **A:** (S)-DPP-0113 [(S)-3c] and **B:** (R)-DPP-0113 [(R)-3c]. (a) Standard sample of (S)-DPP-0113 [(S)-3c] or (R)-DPP-0113 [(R)-3c]; (b) mixture of (S)-DPP-0113 [(S)-3c] or (R)-DPP-0113 [(R)-3c] and HL-60 cell homogenate (just after having been mixed; not incubated); (c) incubated mixture of (S)-DPP-0113 [(S)-3c] or (R)-DPP-0113 [(R)-3c] and HL-60 cell homogenate; (d) standard sample of (R,S)-DPP-0123 [(R,S)-7c], (S,S)-DPP-0123 [(S,S)-7c], (R,R)-DPP-0123 [(R,R)-7c] and (S,R)-DPP-0123 [(S,R)-7c].

all optical isomers of LG190178 (**7d**) showed similar AR-binding affinity, with  $K_i$  values of 1000–1100 nM, suggesting that the exchanged nitrogen atom(s) interacts with some residue(s) in the ligand-binding pocket of AR (entries 24–27 in Table 3).

None of the compounds examined above (**3a–d** and **7a–d**) showed growth-promoting activity on the androgen-dependent cell line SC-3, suggesting they are not androgen agonists, but androgen antagonists,

as reported before.<sup>13</sup> In fact, the (S,S)-isomers of **7a–d**, that is, eutomers for AR-binding, were more potent growth inhibitors of testosterone-induced SC-3 cells than was hydroxyflutamide, which is in accordance with their higher affinity for AR than that of hydroxyflutamide (Table 4). (S,S)-DPP-0123 [(S,S)-7c] showed the most potent activity, with an  $IC_{50}$  value of 4.7 nM, among the compounds listed in Table 4 (entry 4), being almost 40 times more potent than hydroxyflutamide (entry 1).

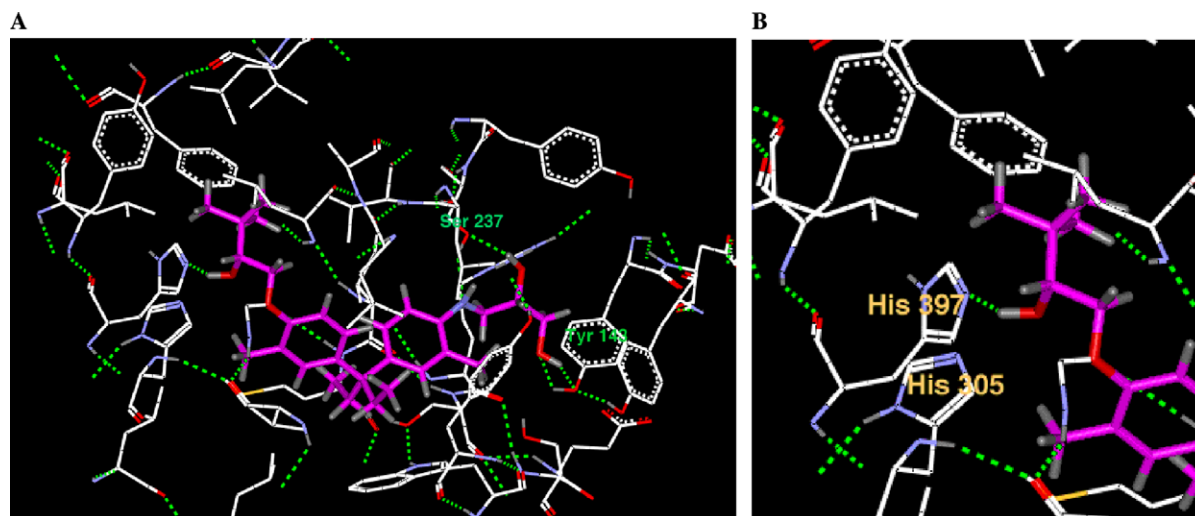


**Figure 5.** Model structure of *(R,S)*-DPP-0123 [(*R,S*)-7c]/VDR–LBD complex. (A) Whole structure of *(R,S)*-DPP-0123 [(*R,S*)-7c] (purple). (B) Magnified view around His 397.

**Table 3.** AR-binding activity of 3,3-diphenylpentane derivatives

Entry	Compound	AR affinity ( $K_i$ , nM)
1	Testosterone	9
2	Hydroxyflutamide	940
3	<i>(R)</i> -DPP-1113 [( <i>R</i> )-3a]	2200
4	<i>(S)</i> -DPP-1113 [( <i>S</i> )-3a]	7400
5	<i>(R)</i> -DPP-1013 [( <i>R</i> )-3b]	1500
6	<i>(S)</i> -DPP-1013 [( <i>S</i> )-3b]	2800
7	DPP-0113 (3c) <sup>a,13</sup>	1170
8	<i>(R)</i> -DPP-0113 [( <i>R</i> )-3c]	3400
9	<i>(S)</i> -DPP-0113 [( <i>S</i> )-3c]	720
10	<i>(R)</i> -DPP-0013 [( <i>R</i> )-3d]	1100
11	<i>(S)</i> -DPP-0013 [( <i>S</i> )-3d]	1800
12	<i>(R,R)</i> -DPP-1123 [( <i>R,R</i> )-7a]	1100
13	<i>(S,R)</i> -DPP-1123 [( <i>S,R</i> )-7a]	1100
14	<i>(R,S)</i> -DPP-1123 [( <i>R,S</i> )-7a]	2300
15	<i>(S,S)</i> -DPP-1123 [( <i>S,S</i> )-7a]	540
16	<i>(R,R)</i> -DPP-1023 [( <i>R,R</i> )-7b]	1200
17	<i>(S,R)</i> -DPP-1023 [( <i>S,R</i> )-7b]	1200
18	<i>(R,S)</i> -DPP-1023 [( <i>R,S</i> )-7b]	910
19	<i>(S,S)</i> -DPP-1023 [( <i>S,S</i> )-7b]	730
20	<i>(R,R)</i> -DPP-0123 [( <i>R,R</i> )-7c]	2500
21	<i>(S,R)</i> -DPP-0123 [( <i>S,R</i> )-7c]	1100
22	<i>(R,S)</i> -DPP-0123 [( <i>R,S</i> )-7c]	1900
23	<i>(S,S)</i> -DPP-0123 [( <i>S,S</i> )-7c]	400
24	<i>(R,R)</i> -LG190178 [( <i>R,R</i> )-7d]	1000
25	<i>(S,R)</i> -LG190178 [( <i>S,R</i> )-7d]	1100
26	<i>(R,S)</i> -LG190178 [( <i>R,S</i> )-7d]	1000
27	<i>(S,S)</i> -LG190178 [( <i>S,S</i> )-7d]	1100

<sup>a</sup> Enantiomeric mixture.

## 6. Structure–activity relationships

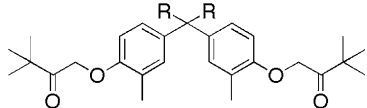
As mentioned above, the pivaloyl derivatives (3a–d) can be regarded as prodrugs for vitamin D<sub>3</sub> agonists, but as

**Table 4.** Androgen–antagonistic activity measured by growth-inhibition of SC-3 cells treated with testosterone

Entry	Compound	SC-3 cell growth inhibition (IC <sub>50</sub> , nM)
1	Hydroxyflutamide	180
2	<i>(S)</i> -DPP-0113 [( <i>S</i> )-3c]	32
3	<i>(S,S)</i> -DPP-1123 [( <i>S,S</i> )-7a]	22
4	<i>(S,S)</i> -DPP-1023 [( <i>S,S</i> )-7b]	4.7
5	<i>(S,S)</i> -DPP-0123 [( <i>S,S</i> )-7c]	55
6	<i>(S,S)</i> -LG190178 [( <i>S,S</i> )-7d]	13

direct-acting androgen antagonists. Among the prepared compounds, *(R,S)*-DPP-1023 [(*R,S*)-7b] and *(S,S)*-DPP-0123 [(*S,S*)-7c] are the most potent vitamin D<sub>3</sub> agonist and androgen antagonist, respectively. The results of our metabolic experiments using HL-60 cell homogenate (vide supra) suggest that, although metabolic reduction of the pivaloyl group of 3a–d, as well as LG190155 (9) and LG190119 (13), which were previously reported by other researchers as VD-bioisoters,<sup>4,5</sup> is necessary to elicit vitamin D<sub>3</sub>-agonistic activity, the reduction easily proceeds in HL-60 cells (Figs. 3 and 4). Thus, it should be possible to assess structure–activity relationships (SAR) for vitamin D<sub>3</sub>-agonistic and androgen–antagonistic activities using HL-60 cell differentiation-induction and SC-3 cell growth inhibition assays, even though the compounds are pivaloyl derivatives. Therefore, we used these assay systems to investigate the SAR concerning the geminal diethyl moiety of the DPP skeleton, that is, compounds 8–14 (Table 5).

Although the order of potency of vitamin D<sub>3</sub>-agonistic activity (estimated as HL-60 cell differentiation induction) and that of androgen–antagonistic activity (estimated as testosterone-induced SC-3 cell growth inhibition) among compounds 8–14 are different, the DPP skeleton (9) seems to be the optimum ligand structure for both VDR and AR (Table 5). Substitution of one or two phenolic oxygen of LG190155 (9) with

**Table 5.** Vitamin D<sub>3</sub>-agonistic and androgen-antagonistic activities of pivaloyl derivatives


	8	9 LG190155 <sup>d</sup>	10	11	12	13 LG190119 <sup>d</sup>	14
HL-60 cell differentiation-inducing activity (EC <sub>50</sub> , nM)	4000	410	Inactive <sup>a</sup>	>10,000	Inactive <sup>a</sup>	2000 <sup>d</sup>	Inactive <sup>a</sup>
SC-3 cell growth inhibitory activity (IC <sub>50</sub> , nM)	3200	1900	15,000	11,000	Inactive <sup>a</sup>	Inactive <sup>a</sup>	Inactive <sup>a</sup>

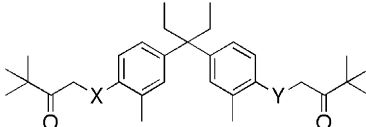
<sup>a</sup> The activity was not observed in the concentration range examined.

nitrogen, that is, DPP-1111 (**15**) and DPP-0111 (**16**), did not apparently affect the activities [Tables 5 (for **9**) and 6 (for **15** and **16**)]. These results suggest that the DPP skeleton is an effective steroid skeleton substitute, and the nuclear receptor selectivity of the compounds can be attributed to the structure(s) of the side chain(s). In fact, on the basis of this consideration, we recently reported the successful creation of specific ligands for other nuclear receptors, including farnesoid X receptor (FXR) and peroxisome proliferator-activated receptor (PPAR), based on the DPP skeleton.<sup>34</sup>

The pivaloyl derivatives (**3a–d**) can be regarded as intrinsically AR-selective ligands, because their reduction was shown to be necessary to bind VDR (vide supra). Non-metabolizable analog(s) would be AR-specific ligand(s). The reduced analogs **7a–d** are direct ligands for both VDR and AR. Concerning **7a–c**, the (*R,S*)- and (*S,S*)-isomers are the eutomers for VDR and AR, respectively. For **7d**, the (*R,S*)- and (*S,S*)-isomers are comparably potent VDR agonists. The (*S,R*)-isomers are generally the weakest 1,25-VD<sub>3</sub> agonists among all of the compounds **7a–d**. In other words, the stereochemistry at the side chain is critical for the selectivity for nuclear receptors.

All the optical isomers of LG190178 (**7d**) possess similar affinity for AR, with *K<sub>i</sub>* values of 1000 to 1100 (entries 24–27 in Table 3). The replacement of one or two phenolic oxygen atom(s) with nitrogen atom(s) in (*S,S*)-LG190178 [(*S,S*)-**7d**], which has a *K<sub>i</sub>* value of 1100 nM, enhances the AR-binding affinity of the compounds, that is, (*S,S*)-**7a–c** have *K<sub>i</sub>* values of 400–730 nM, suggesting that there is an interaction between the nitrogen atom(s) and some residue(s) in the ligand-binding pocket of AR. We are planning computer-assisted docking studies of these AR ligands and the AR ligand-binding pocket to clarify this Table 6.

Comparison of the *K<sub>i</sub>* values of **7a–d** toward VDR- and AR-binding (Tables 2 and 3) indicates that the (*R,S*)-isomers selectively bind to VDR with 8.6–95.8 times higher affinity than that for AR (entries 3, 7, 11, and 15 in Table 7). The selectivity of the (*S,S*)-isomers is not so clear. (*S,S*)-DPP-1123 [(*S,S*)-**7a**] and (*S,S*)-

**Table 6.** Vitamin D<sub>3</sub>-agonistic and androgen-antagonistic activities of DPP-1111 (**15**) and DPP-0111 (**16**)


	X = Y = N DPP-1111 <b>15</b>	X = O, Y = N DPP-0111 <b>16</b>
HL-60 cell differentiation-inducing activity (EC <sub>50</sub> , nM)	450	450
SC-3 cell growth inhibitory activity (IC <sub>50</sub> , nM)	1000	1200

DPP-0123 [(*S,S*)-**7c**] are dual ligands which bind to both AR and VDR with similar *K<sub>i</sub>* values (350–540 nM) (Tables 2, 3 and 7). The (*S,R*)-isomers of **7a–d**, except that of **7b**, are also regarded as dual ligands, though their affinity for both VDR and AR is moderate with *K<sub>i</sub>* values of 580–1100 nM. Among the compounds prepared in this study (*S,S*)-DPP-0123 [(*S,S*)-**7c**] is a potent ligand for AR, while (*R,S*)-DPP-1023 [(*R,S*)-**7b**] is the best ligand for VDR. A group of Eli Lilly & Co. reported comprehensive studies of the related compounds as VDR modulators.<sup>35–37</sup> Further structure-activity relationship studies, as well as further work to develop superior ligands for VDR, AR and other nuclear receptors based on the DPP skeleton are in progress.

## 7. Experimental

### 7.1. 1-[4-[3-(4-Amino-3-methylphenyl)pentan-3-yl]-2-methylphenylamino]-3,3-dimethylbutan-2-one (DPP-1101: **2**)

To a stirred solution of **1** (84.2 mg, 0.298 mmol), potassium iodide (49.5 mg, 0.298 mmol), and triethylamine (42.0 μL, 0.298 mmol) in DMF (1.5 mL) was added 1-chloropinacolone (39.2 μL, 0.298 mmol). The reaction mixture was stirred at room temperature for 26 h, then

**Table 7.** Selectivity of **7a–d** for the binding to VDR and AR

Entry	Compound	Selectivity	Selectivity toward VDR [ $K_i$ for AR/ $K_i$ for VDR] or AR [ $K_i$ for VDR/ $K_i$ for AR]
1	( <i>R,R</i> )-DPP-1123 [( <i>R,R</i> )- <b>7a</b> ]	VDR	5.8-fold VDR-selective
2	( <i>S,R</i> )-DPP-1123 [( <i>S,R</i> )- <b>7a</b> ]	Dual (VDR)	1.9-fold VDR-selective
3	( <i>R,S</i> )-DPP-1123 [( <i>R,S</i> )- <b>7a</b> ]	VDR	19.2-fold VDR-selective
4	( <i>S,S</i> )-DPP-1123 [( <i>S,S</i> )- <b>7a</b> ]	Dual (VDR)	1.5-fold VDR-selective
5	( <i>R,R</i> )-DPP-1023 [( <i>R,R</i> )- <b>7b</b> ]	VDR	8.0-fold VDR-selective
6	( <i>S,R</i> )-DPP-1023 [( <i>S,R</i> )- <b>7b</b> ]	VDR	6.7-fold VDR-selective
7	( <i>R,S</i> )-DPP-1023 [( <i>R,S</i> )- <b>7b</b> ]	VDR	95.8-fold VDR-selective
8	( <i>S,S</i> )-DPP-1023 [( <i>S,S</i> )- <b>7b</b> ]	VDR	36.5-fold VDR-selective
9	( <i>R,R</i> )-DPP-0123 [( <i>R,R</i> )- <b>7c</b> ]	VDR	7.4-fold VDR-selective
10	( <i>S,R</i> )-DPP-0123 [( <i>S,R</i> )- <b>7c</b> ]	Dual	1.0
11	( <i>R,S</i> )-DPP-0123 [( <i>R,S</i> )- <b>7c</b> ]	VDR	8.6-fold VDR-selective
12	( <i>S,S</i> )-DPP-0123 [( <i>S,S</i> )- <b>7c</b> ]	Dual (AR)	1.1-fold AR-selective
13	( <i>R,R</i> )-LG190178 [( <i>R,R</i> )- <b>7d</b> ]	VDR	3.1-fold VDR-selective
14	( <i>S,R</i> )-LG190178 [( <i>S,R</i> )- <b>7d</b> ]	Dual (VDR)	1.5-fold VDR-selective
15	( <i>R,S</i> )-LG190178 [( <i>R,S</i> )- <b>7d</b> ]	VDR	83.3-fold VDR-selective
16	( <i>S,S</i> )-LG190178 [( <i>S,S</i> )- <b>7d</b> ]	VDR	100-fold VDR-selective

saturated  $\text{NH}_4\text{Cl}$  aq was added, and the whole was extracted with  $\text{CH}_2\text{Cl}_2$ . The organic layer was washed with brine, dried over  $\text{MgSO}_4$ , and concentrated. The resulting residue was purified by silica gel chromatography (ethyl acetate/hexane = 1:4) to afford **2** (43.7 mg, 0.115 mmol, 39%) as a colorless oil.  $^1\text{H}$  NMR (500 MHz,  $\text{CDCl}_3/\delta$ ): 6.94 (dd,  $J = 8.1, 2.1$  Hz, 1H), 6.85–6.82 (m, 3H), 6.56 (d,  $J = 8.1$  Hz, 1H), 6.40 (d,  $J = 8.1$  Hz, 1H), 4.13 (s, 2H), 3.51 (br s, 2H), 2.16 (s, 3H), 2.11 (s, 3H), 1.99 (q,  $J = 7.3$  Hz, 4H), 1.24 (s, 9H), 0.60 (t,  $J = 7.3$  Hz, 6H). HRMS (FAB,  $\text{M}^+$ ) calcd for  $\text{C}_{25}\text{H}_{36}\text{N}_2\text{O}$ , 380.2828, found 380.2839.

## 7.2. 1-(4-{3-[4-(2,3-Dihydroxypropylamino)-3-methylphenyl]pentan-3-yl}-2-methylphenylamino)-3,3-dimethylbutan-2-one (DPP-1113: **3a**)

To a stirred solution of DPP-1101 (**2**) (21.4 mg, 56.2  $\mu\text{mol}$ ) in EtOH (0.3 mL) was added (*S*)-glycidol (4.5  $\mu\text{L}$ , 67.4 mmol) at 85 °C. The reaction mixture was stirred for 18 h, then concentrated. The residue was purified by silica gel chromatography (ethyl acetate/hexane = 1:1) to afford (*R*)-DPP-1113 [(*R*)-**3a**] (8.9 mg, 19.6  $\mu\text{mol}$ , 35%) as a colorless oil. The same procedure, but starting from DPP-1101 (**2**) (20.8 mg, 54.7  $\mu\text{mol}$ ) and with (*R*)-glycidol (4.3  $\mu\text{L}$ , 65.6  $\mu\text{mol}$ ) instead of (*S*)-glycidol, gave (*S*)-**3a** (6.5 mg, 14.3  $\mu\text{mol}$ , 26%) as a colorless oil.

**7.2.1. (*R*)-DPP-1113 [(*R*)-**3a**].**  $^1\text{H}$  NMR (500 MHz,  $\text{CDCl}_3/\delta$ ): 6.95 (d,  $J = 8.6$  Hz, 2H), 6.85 (s, 2H), 6.55 (d,  $J = 8.1$  Hz, 1H), 6.40 (d,  $J = 8.6$  Hz, 1H), 4.13 (s, 2H), 4.01 (m, 1H), 3.84–3.81 (m, 2H), 3.34–3.21 (m, 2H), 2.16 (s, 3H), 2.10 (s, 3H), 2.00 (q,  $J = 7.3$  Hz, 4H), 1.24 (s, 9H), 0.60 (t,  $J = 7.3$  Hz, 6H).  $^{13}\text{C}$  NMR (125 MHz,  $\text{CDCl}_3/\delta$ ): 211.7, 143.2, 142.5, 138.7, 137.9, 130.2, 130.2, 126.5, 126.4, 122.0, 121.6, 109.6, 109.0, 70.2, 65.0, 48.8, 48.1, 46.9, 43.1, 29.7, 29.3, 26.5, 17.9, 17.7, 8.5. HRMS (FAB,  $\text{M}^+$ ) calcd for  $\text{C}_{28}\text{H}_{42}\text{N}_2\text{O}_3$ , 454.3195, found 454.3194.

**7.2.2. (*S*)-DPP-1113 [(*S*)-**3a**].** NMR spectra were the same as those of (*R*)-DPP-1113 [(*R*)-**3a**]. HRMS (FAB,  $\text{M}^+$ ) calcd for  $\text{C}_{28}\text{H}_{42}\text{N}_2\text{O}_3$ , 454.3195, found 454.3184.

## 7.3. 3-{4-[3-(4-Amino-3-methylphenyl)pentan-3-yl]-2-methylphenoxy}propane-1,2-diol (DPP-1003: **5**)

To a stirred solution of DPP-0100 (**4**) (1.10 g, 3.88 mmol) in DMF (15 mL) were added cesium fluoride (177 mg, 1.16 mmol) and (*R*)-glycidol (386  $\mu\text{L}$ , 5.82 mmol) at 85 °C. The reaction mixture was stirred for 9 h, then water was added, and the whole was extracted with ethyl acetate. The organic layer was washed with brine, dried over  $\text{MgSO}_4$ , and concentrated. The residue was purified by silica gel chromatography (ethyl acetate/hexane = 1:1) to afford (*R*)-DPP-1003 [(*R*)-**5**] (1.06 g, 2.97 mmol, 77%) as a white foam. The same procedure, but starting from DPP-0100 (**4**) (117 mg, 0.413 mmol) and with (*S*)-glycidol (41.1  $\mu\text{L}$ , 0.620 mmol) instead of (*R*)-glycidol, gave (*S*)-DPP-1003 [(*S*)-**5**] (134 mg, 0.374 mmol, 91%) as a white foam.

**7.3.1. (*R*)-DPP-1003 [(*R*)-**5**].**  $^1\text{H}$  NMR (500 MHz,  $\text{CDCl}_3/\delta$ ): 6.97 (dd,  $J = 8.5, 2.1$  Hz, 2H), 6.93 (d,  $J = 2.1$  Hz, 2H), 6.82–6.80 (m, 2H), 6.69 (d,  $J = 8.1$  Hz, 2H), 6.57 (d,  $J = 8.1$  Hz, 2H), 4.11 (m, 1H), 4.04–4.03 (m, 2H), 3.84–3.79 (m, 2H), 3.48 (br, 2H), 2.55 (br, 1H), 2.16 (s, 3H), 2.12 (s, 3H), 2.00 (q,  $J = 7.3$  Hz, 4H), 0.59 (t,  $J = 7.3$  Hz, 6H). MS (FAB,  $\text{M}^+$ )  $m/z$  357.

**7.3.2. (*S*)-DPP-1003 [(*R*)-**5**].** MS (FAB,  $\text{M}^+$ )  $m/z$  357. NMR spectra were the same as those of (*R*)-DPP-1103 [(*R*)-**5**].

## 7.4. 1-(4-{3-[4-(2,3-Dihydroxypropoxy)-3-methylphenyl]pentan-3-yl}-2-methylphenylamino)-3,3-dimethylbutan-2-one (DPP-1013: **3b**)

To a stirred solution of (*R*)-DPP-1003 [(*R*)-**5**] (148 mg, 0.413 mmol), potassium iodide (103 mg, 0.620 mmol),

and triethylamine (86  $\mu$ L, 0.620 mmol) in DMF (2 mL) was added 1-chloropinacolone (59.7  $\mu$ L, 0.454 mmol). The reaction mixture was stirred at room temperature for 17 h, then saturated  $\text{NH}_4\text{Cl}$  aq was added, and the whole was extracted with ethyl acetate. The organic layer was washed with brine, dried over  $\text{MgSO}_4$ , and concentrated. The resulting residue was purified by silica gel chromatography (ethyl acetate/hexane = 1:1) to afford (*R*)-DPP-1013 [(*R*)-**3b**] (90.6 mg, 0.199 mmol, 48%) as a white foam. The same procedure, but starting from (*S*)-DPP-1003 [(*S*)-**5**] (124 mg, 0.345 mmol) instead of (*R*)-DPP-1003 [(*R*)-**5**], gave (*S*)-DPP-1013 [(*S*)-**3b**] (59.2 mg, 0.130 mmol, 38%) as a white foam.

**7.4.1. (*R*)-DPP-1013 [(*R*)-**3b**].**  $^1\text{H}$  NMR (500 MHz,  $\text{CDCl}_3/\delta$ ): 7.01–6.92 (m, 3H), 6.83 (s, 1H), 6.69 (d,  $J = 8.1$  Hz, 1H), 6.40 (d,  $J = 8.1$  Hz, 1H), 4.14–4.10 (m, 3H), 4.05–4.03 (m, 2H), 3.86–3.76 (m, 2H), 2.16 (s, 6H), 2.01 (q,  $J = 7.3$  Hz, 4H), 1.24 (s, 9H), 0.59 (t,  $J = 7.3$  Hz, 6H).  $^{13}\text{C}$  NMR (125 MHz,  $\text{CDCl}_3/\delta$ ): 211.7, 153.9, 142.6, 141.8, 137.6, 130.7, 130.1, 126.4, 126.3, 125.2, 121.6, 110.0, 109.0, 70.4, 69.2, 63.9, 48.8, 48.3, 43.1, 29.3, 26.5, 17.7, 16.6, 8.5. HRMS (FAB,  $\text{M}^+$ ) calcd for  $\text{C}_{28}\text{H}_{41}\text{NO}_4$ , 455.3036, found 455.3036.

**7.4.2. (*S*)-DPP-1013 [(*S*)-**3b**].** NMR spectra were the same as those of (*R*)-DPP-1013 [(*R*)-**3b**]. HRMS (FAB,  $\text{M}^+$ ) calcd for  $\text{C}_{28}\text{H}_{41}\text{NO}_4$ , 455.3036, found 455.3058.

#### 7.5. 1-{4-[3-(4-Amino-3-methylphenyl)pentan-3-yl]-2-methylphenoxy}-3,3-dimethylbutan-2-one (DPP-1001: **6**)

To a stirred solution of NaH (85.2 mg, 50%, 1.77 mmol) in DMF (7 mL) was added DPP-0100 (**4**) (503 mg, 1.77 mmol) and the mixture was stirred for 30 min. 1-Chloropinacolone (256  $\mu$ L, 1.95 mmol) was added, and stirring was continued for 21 h. The reaction mixture was partitioned between  $\text{H}_2\text{O}$  and ethyl acetate. The organic layer was washed with brine, dried over  $\text{MgSO}_4$ , and concentrated. The resulting residue was purified by silica gel chromatography (ethyl acetate/hexane = 1:4) to afford DPP-1001 (**6**) (656 mg, 1.72 mmol, 97%) as white crystals.  $^1\text{H}$  NMR (500 MHz,  $\text{CDCl}_3/\delta$ ): 6.93 (s, 1H), 6.91 (dd,  $J = 8.5, 2.6$  Hz, 1H), 6.82–6.80 (m, 2H), 6.56 (d,  $J = 8.1$  Hz, 1H), 6.49 (d,  $J = 7.7$  Hz, 1H), 4.82 (s, 2H), 3.47 (s, 2H), 2.23 (s, 3H), 2.12 (s, 3H), 1.99 (q,  $J = 7.3$  Hz, 4H), 1.25 (s, 9H), 0.59 (t,  $J = 7.3$  Hz, 6H). MS (FAB,  $\text{M}^+$ )  $m/z$  381.

#### 7.6. 1-(4-{3-[4-(2,3-Dihydroxypropylamino)-3-methylphenyl]pentan-3-yl}-2-methylphenoxy)-3,3-dimethylbutan-2-one (DPP-0113: **3c**)

To a stirred solution of DPP-1001 (**6**) (47.2 mg, 0.124 mmol) in ethanol (0.6 mL) was added (*S*)-glycidol (9.8  $\mu$ L, 0.149 mmol). The reaction mixture was stirred at 75  $^\circ\text{C}$  for 22 h, then concentrated, and the residue was purified by silica gel chromatography (ethyl acetate/hexane = 1:1–1:0) to afford (*R*)-DPP-0113 [(*R*)-**3c**] (38.4 mg, 84.3  $\mu$ mol, 68%) as a white foam.

The same procedure, but starting from DPP-1001 (**6**) (50.1 mg, 0.131 mmol) and with (*R*)-glycidol (10.4  $\mu$ L,

0.157 mmol) instead of (*S*)-glycidol, gave (*S*)-DPP-0113 [(*S*)-**3c**] (41.3 mg, 90.6  $\mu$ mol, 69%) as a white foam.

**7.6.1. (*R*)-DPP-0113 [(*R*)-**3c**].**  $^1\text{H}$  NMR (500 MHz,  $\text{CDCl}_3/\delta$ ): 6.94–6.89 (m, 3H), 6.82 (d,  $J = 2.1$  Hz, 1H), 6.55 (d,  $J = 8.5$  Hz, 1H), 6.49 (d,  $J = 8.1$  Hz, 1H), 4.83 (s, 2H), 4.01 (m, 1H), 3.82 (dd,  $J = 11.1, 3.4$  Hz, 1H), 3.70–3.66 (m, 1H), 3.33 (dd,  $J = 12.8, 4.3$  Hz, 1H), 3.25–3.21 (m, 1H), 2.23 (s, 3H), 2.11 (s, 3H), 2.00 (q,  $J = 7.3$  Hz, 4H), 1.25 (s, 9H), 0.59 (t,  $J = 7.3$  Hz, 6H).  $^{13}\text{C}$  NMR (125 MHz,  $\text{CDCl}_3$ )  $\delta$  210.1, 153.9, 143.3, 141.8, 138.3, 130.8, 130.2, 126.5, 126.1, 125.9, 122.1, 110.2, 109.6, 70.3, 69.7, 65.0, 48.3, 46.9, 43.2, 29.3, 26.4, 17.8, 16.7, 8.5. HRMS (FAB,  $\text{M}^+$ ) calcd for  $\text{C}_{28}\text{H}_{41}\text{NO}_4$ , 455.3036, found 455.3037. HPLC: ChiralPak AD, IPA/hexane = 1:9, 0.5 mL/min,  $t_R = 22.6$  min, 96% ee.

**7.6.2. (*S*)-DPP-0113 [(*S*)-**3c**].** NMR equal to (*R*)-DPP-0113 [(*R*)-**3c**]. HRMS (FAB,  $\text{M}^+$ ) calcd for  $\text{C}_{28}\text{H}_{41}\text{NO}_4$ , 455.3036, found 455.3032. HPLC: ChiralPak AD, IPA/hexane = 1:9, 0.5 mL/min,  $t_R = 24.8$  min, 96% ee.

#### 7.7. General procedure for reduction of the carbonyl group of **3a–d**

To a stirred mixture of **3** in MeOH (0.1 M) was added sodium borohydride (1.5 equiv) at 0  $^\circ\text{C}$  and stirring was continued at room temperature for 1 h. To the reaction mixture was added saturated  $\text{NH}_4\text{Cl}$  aq, and the mixture was extracted with ethyl acetate. The organic layer was washed with brine, dried over  $\text{MgSO}_4$ , and concentrated to afford compound **7**. The diastereomeric mixture was separated by chiral HPLC [Chiralpak AD-H (4.6  $\times$  250 mm), IPA/hexane = 1:4, 0.50 mL/min].

#### 7.8. 3-(4-{3-[4-(2-Hydroxy-3,3-dimethylbutylamino)-3-methylphenyl]pentan-3-yl}-2-methylphenoxy)-propane-1,2-diol (DPP-1123: **7a**)

**7.8.1. (*R,R*)-DPP-1123 [(*R,R*)-**7a**].** Colorless oil.  $^1\text{H}$  NMR (500 MHz,  $\text{CDCl}_3/\delta$ ): 6.96–6.93 (m, 2H), 6.85 (s, 2H), 6.54 (d,  $J = 8.6$  Hz, 2H), 4.01 (m, 1H), 3.84–3.81 (m, 1H), 3.70–3.66 (m, 1H), 3.52 (d,  $J = 10.3$  Hz, 1H), 3.37 (dd,  $J = 12.4, 2.6$  Hz, 1H), 3.34–3.21 (m, 2H), 2.99 (dd,  $J = 12.4, 10.3$  Hz, 1H), 2.10 (s, 6H), 1.99 (q,  $J = 7.3$  Hz, 4H), 0.99 (s, 9H), 0.60 (t,  $J = 7.3$  Hz, 6H).  $^{13}\text{C}$  NMR (125 MHz,  $\text{CDCl}_3/\delta$ ): 143.6, 143.2, 138.7, 138.3, 130.2, 130.1, 126.5, 126.5, 122.0, 122.0, 109.5, 109.5, 76.8, 70.2, 65.0, 48.1, 46.9, 45.8, 34.1, 29.7, 29.3, 25.8, 17.9, 8.5. HRMS (FAB,  $\text{M}+\text{H}^+$ ) calcd for  $\text{C}_{28}\text{H}_{45}\text{N}_2\text{O}_3$ , 457.3430, found 457.3443. HPLC: Chiralpak AD-H (4.6  $\times$  250 mm), IPA/hexane = 1:4, 0.50 mL/min,  $t_R = 12.3$  min.

**7.8.2. (*S,R*)-DPP-1123 [(*S,R*)-**7a**].** Colorless oil. NMR spectra were the same as those of (*R,R*)-DPP-1123 [(*R,R*)-**7a**]. HRMS (FAB,  $\text{M}^+$ ) calcd for  $\text{C}_{28}\text{H}_{44}\text{N}_2\text{O}_3$ , 456.3352, found 456.3384. HPLC: Chiralpak AD-H (4.6  $\times$  250 mm), IPA/hexane = 1:4, 0.50 mL/min,  $t_R = 13.9$  min.

**7.8.3. (R,S)-DPP-1123 [(R,S)-7a].** Colorless oil. NMR spectra were the same as those of (R,R)-DPP-1123 [(R,R)-7a]. HRMS (FAB, M+H<sup>+</sup>) calcd for C<sub>28</sub>H<sub>45</sub>N<sub>2</sub>O<sub>3</sub>, 457.3430, found 457.3451. HPLC: Chiralpak AD-H (4.6 × 250 mm), IPA/hexane = 1:4, 0.50 mL/min, t<sub>R</sub> = 12.6 min.

**7.8.4. (S,S)-DPP-1123 [(S,S)-7a].** Colorless oil. NMR spectra were the same as those of (R,R)-DPP-1123 [(R,R)-7a]. HRMS (FAB, M+H<sup>+</sup>) calcd for C<sub>28</sub>H<sub>45</sub>N<sub>2</sub>O<sub>3</sub>, 457.3430, found 457.3424. HPLC: Chiralpak AD-H (4.6 × 250 mm), IPA/hexane = 1:4, 0.50 mL/min, t<sub>R</sub> = 14.6 min.

**7.9. 3-(4-{3-[4-(2-Hydroxy-3,3-dimethylbutylamino)-3-methylphenyl]pentan-3-yl}-2-methylphenyl-amino)propane-1,2-diol (DPP-1023: 7b)**

**7.9.1. (R,R)-DPP-1023 [(R,R)-7b].** Colorless oil. <sup>1</sup>H NMR (500 MHz, CDCl<sub>3</sub>/δ): 7.01–6.91 (m, 3H), 6.82 (s, 1H), 6.69 (d, J = 8.6 Hz, 1H), 6.54 (d, J = 8.6 Hz, 1H), 4.13–4.10 (m, 1H), 4.03 (d, J = 5.6 Hz, 2H), 3.86–3.76 (m, 2H), 3.53 (d, J = 8.1 Hz, 1H), 3.37 (d, J = 12.4 Hz, 1H), 2.99 (dd, J = 12.4, 8.1 Hz, 2H), 2.16 (s, 3H), 2.10 (s, 3H), 2.01 (q, J = 7.3 Hz, 4H), 0.99 (s, 9H), 0.59 (t, J = 7.3 Hz, 6H). <sup>13</sup>C NMR (125 MHz, CDCl<sub>3</sub>/δ): 153.8, 143.6, 141.8, 138.0, 130.7, 130.1, 126.4, 126.3, 125.2, 122.1, 109.9, 109.5, 77.5, 70.4, 69.1, 63.9, 48.2, 45.8, 34.1, 29.2, 25.8, 17.9, 16.6, 8.5. HRMS (FAB, M<sup>+</sup>) calcd for C<sub>28</sub>H<sub>43</sub>NO<sub>4</sub>, 457.3192, found 457.3169. HPLC: Chiralpak AD-H (4.6 × 250 mm), IPA/hexane = 1:4, 0.50 mL/min, t<sub>R</sub> = 14.5 min.

**7.9.2. (S,R)-DPP-1023 [(S,R)-7b].** Colorless oil. NMR spectra were the same as those of (R,R)-DPP-1023 [(R,R)-7b]. HRMS (FAB, M<sup>+</sup>) calcd for C<sub>28</sub>H<sub>43</sub>NO<sub>4</sub>, 457.3192, found 457.3184. HPLC: Chiralpak AD-H (4.6 × 250 mm), IPA/hexane = 1:4, 0.50 mL/min, t<sub>R</sub> = 16.8 min.

**7.9.3. (R,S)-DPP-1023 [(R,S)-7b].** Colorless oil. NMR spectra were the same as those of (R,R)-DPP-1023 [(R,R)-7b]. HRMS (FAB, M<sup>+</sup>) calcd for C<sub>28</sub>H<sub>43</sub>NO<sub>4</sub>, 457.3192, found 457.3181. HPLC: Chiralpak AD-H (4.6 × 250 mm), IPA/hexane = 1:4, 0.50 mL/min, t<sub>R</sub> = 14.3 min.

**7.9.4. (S,S)-DPP-1023 [(S,S)-7b].** Colorless oil. NMR spectra were the same as those of (R,R)-DPP-1023 [(R,R)-7b]. HRMS (FAB, M<sup>+</sup>) calcd for C<sub>28</sub>H<sub>43</sub>NO<sub>4</sub>, 457.3192, found 457.3196. HPLC: Chiralpak AD-H (4.6 × 250 mm), IPA/hexane = 1:4, 0.50 mL/min, t<sub>R</sub> = 16.7 min.

**7.10. 3-(4-{3-[4-(2-Hydroxy-3,3-dimethylbutoxy)-3-methylphenyl]pentan-3-yl}-2-methylphenylamino)-propane-1,2-diol (DPP-0123: 7c)**

**7.10.1. (R,R)-DPP-0123 [(R,R)-7c].** Colorless oil. <sup>1</sup>H NMR (500 MHz, CDCl<sub>3</sub>/δ): 6.97–6.92 (m, 3H), 6.83 (d, J = 1.7 Hz, 1H), 6.69 (d, J = 8.6 Hz, 1H), 6.55 (d, J = 8.2 Hz, 1H), 4.10–4.07 (dd, J = 9.4, 2.6 Hz, 1H),

4.01 (m, 1H), 3.87–3.81 (m, 2H), 3.71–3.67 (m, 2H), 3.33 (dd, J = 12.8, 4.3 Hz, 1H), 3.25–3.21 (m, 1H), 2.17 (s, 3H), 2.11 (s, 3H), 2.01 (q, J = 7.3 Hz, 4H), 1.01 (s, 9H), 0.60 (t, J = 7.3 Hz, 6H). <sup>13</sup>C NMR (125 MHz, CDCl<sub>3</sub>/δ): 154.2, 143.3, 141.4, 138.3, 130.7, 130.2, 126.4, 126.2, 122.1, 110.1, 109.6, 76.8, 70.3, 69.2, 65.0, 48.3, 46.9, 33.6, 29.3, 26.1, 17.8, 16.6, 8.5. RMS (FAB, M<sup>+</sup>) calcd for C<sub>28</sub>H<sub>43</sub>NO<sub>4</sub>, 457.3192, found 457.3169. HPLC: Chiralpak AD-H (4.6 × 250 mm), IPA/hexane = 3:7, 0.50 mL/min, t<sub>R</sub> = 9.9 min.

**7.10.2. (S,R)-DPP-0123 [(S,R)-7c].** Colorless oil. NMR spectra were the same as those of (R,R)-DPP-0123 [(R,R)-7c]. HRMS (FAB, M<sup>+</sup>) calcd for C<sub>28</sub>H<sub>43</sub>NO<sub>4</sub>, 457.3192, found 457.3191. HPLC: Chiralpak AD-H (4.6 × 250 mm), IPA/hexane = 3:7, 0.50 mL/min, t<sub>R</sub> = 15.9 min.

**7.10.3. (R,S)-DPP-0123 [(R,S)-7c].** Colorless oil. NMR spectra were the same as those of (R,R)-DPP-0123 [(R,R)-7c]. HRMS (FAB, M<sup>+</sup>) calcd for C<sub>28</sub>H<sub>43</sub>NO<sub>4</sub>, 457.3192, found 457.3199. HPLC: Chiralpak AD-H (4.6 × 250 mm), IPA/hexane = 3:7, 0.50 mL/min, t<sub>R</sub> = 9.8 min.

**7.10.4. (S,S)-DPP-0123 [(S,S)-7c].** Colorless oil. NMR spectra were the same as those of (R,R)-DPP-0123 [(R,R)-7c]. HRMS (FAB, M<sup>+</sup>) calcd for C<sub>28</sub>H<sub>43</sub>NO<sub>4</sub>, 457.3192, found 457.3212. HPLC: Chiralpak AD-H (4.6 × 250 mm), IPA/hexane = 3:7, 0.50 mL/min, t<sub>R</sub> = 16.1 min.

**7.11. 3-(4-{3-[4-(2-Hydroxy-3,3-dimethylbutoxy)-3-methylphenyl]pentan-3-yl}-2-methylphenylamino)-propane-1,2-diol (LG190178: 7d)**

**7.11.1. (R,R)-LG190178 [(R,R)-7d].** Colorless oil. NMR spectra were the same as those of the diastereomeric mixture of LG190178 given in the literature.<sup>4</sup> HRMS (FAB, M<sup>+</sup>) calcd for C<sub>28</sub>H<sub>42</sub>O<sub>5</sub>, 458.3032, found 458.3025. HPLC: Chiralpak AD-H (4.6 × 250 mm), IPA/hexane = 1:3, 0.50 mL/min, t<sub>R</sub> = 9.5 min.

**7.11.2. (S,R)-LG190178 [(S,R)-7d].** Colorless oil. NMR spectra were the same as those of (R,R)-LG190178 [(R,R)-7d]. HRMS (FAB, M<sup>+</sup>) calcd for C<sub>28</sub>H<sub>42</sub>O<sub>5</sub>, 458.3032, found 458.3031. HPLC: Chiralpak AD-H (4.6 × 250 mm), IPA/hexane = 1:3, 0.50 mL/min, t<sub>R</sub> = 14.8 min.

**7.11.3. (R,S)-LG190178 [(R,S)-7d].** Colorless oil. NMR spectra were the same as those of (R,R)-LG190178 [(R,R)-7d]. HRMS (FAB, M<sup>+</sup>) calcd for C<sub>28</sub>H<sub>42</sub>O<sub>5</sub>, 458.3032, found 458.3042. HPLC: Chiralpak AD-H (4.6 × 250 mm), IPA/hexane = 1:3, 0.50 mL/min, t<sub>R</sub> = 10.4 min.

**7.11.4. (S,S)-LG190178 [(S,S)-7d].** Colorless oil. NMR spectra were the same as those of (R,R)-LG190178 [(R,R)-7d]. HRMS (FAB, M<sup>+</sup>) calcd for C<sub>28</sub>H<sub>42</sub>O<sub>5</sub>, 458.3032, found 458.3042. HPLC: Chiralpak AD-H (4.6 × 250 mm), IPA/hexane = 1:3, 0.50 mL/min, t<sub>R</sub> = 16.2 min.

### 7.12. Evaluation of VDR-binding affinity

Bovine thymus VDR was obtained from Yamasa Biochemical (Choshi, Chiba, Japan) and dissolved in 40 mL of 0.05 M phosphate buffer (pH 7.4) containing 0.3 M KCl, and 1 mM dithiothreitol. Then 0.2 mL of this solution was mixed with 40 nM (26,27-methyl-<sup>3</sup>H)-1,25-VD<sub>3</sub> (Amersham Biosciences Corp.) dissolved in 5 μL of DMSO, and various concentrations of test compound dissolved in 5 μL of DMSO, and the mixture was incubated for 15 h at 4 °C. Then dextran-coated charcoal (0.5 w/v% in phosphate buffer) was added for 20 min, followed by centrifugation at 3000 rpm for 10 min at 4 °C. The supernatant was dissolved in scintillation cocktail (Atomlight, Perkin-Elmer) and the radioactivity was counted with a liquid scintillation counter (Beckman, model 6000LL). The relative binding affinity of the test compounds for VDR was calculated from the concentration necessary to displace 50% of (26,27-methyl-<sup>3</sup>H)-1,25-VD<sub>3</sub> from VDR. Based on the relative affinity thus measured for 1,25-VD<sub>3</sub>, the inhibition constant ( $K_i$ ) values of the test compounds were evaluated. A typical set of values is presented in Table 2.

### 7.13. Measurement of vitamin D<sub>3</sub>-agonistic activity by means of HL-60 cell differentiation induction

The human promyelocytic leukemia cell line HL-60 was purchased from a cell bank (Japanese Cancer Research Resources Bank, cell#: JCRB0085). HL-60 cells were cultured in RPMI-1640 (Life Technologies) medium supplemented with 10% heat-inactivated fetal bovine serum (FBS). The cell concentration at seeding was adjusted to  $3 \times 10^3$  cells/mL and the seeding volume was 1 mL/well. To assess the vitamin D<sub>3</sub>-agonistic activity of the test compounds, the HL-60 cells in the presence or absence of 1,25-VD<sub>3</sub> (a positive control) or a test compound (added to the culture in 1 mL of ethanol solution) were incubated for 96 h at 37 °C in a humidified atmosphere of 5% CO<sub>2</sub>/air without medium change. After incubation, the nitroblue tetrazolium (NBT)-reducing activity of the HL-60 cells was measured. The HL-60 cells were collected by centrifugation, washed with phosphate-buffered saline (PBS), and re-suspended in the medium. To the cell suspension was added NBT (Tokyo Kasei Kogyo) and 12-*O*-tetradecanoylphorbol-13-acetate (TPA, Wako). Final concentrations of NBT and TPA were 0.1% and 100 ng/mL, respectively. Then, the mixture was incubated at 37 °C for 25 min, and cells were collected by centrifugation and re-suspended in PBS. Cytospin smears were prepared, counter-staining of nuclei was done with Kemechrot solution, and the ratio of NBT-positive cells was counted under a microscope. Of course, the percentage values differed from experiment to experiment, but the results were basically reproducible. A typical set of ED<sub>50</sub> values is presented in Table 2.

### 7.14. Evaluation of AR-binding affinity

Binding affinities of the test compounds for hAR (human androgen receptor) were measured in competition experiments using [<sup>3</sup>H]testosterone and cytosolic frac-

tion of hAR-LBD (hAR ligand-binding domain)-transformed *Escherichia coli* as described previously.<sup>28–31</sup> A hAR-LBD expression plasmid vector which encodes GST-hARLBD (627–919 aa, EF domain) fusion protein under the *lac* promoter (provided by Prof. S. Kato, University of Tokyo) was transfected into *E. coli* strain *HB-101*. An overnight culture (10 mL) of the bacteria was added to 1 L of LB medium and incubated at 27 °C until the optical density reached 0.6–0.7 at 600 nm. Following the addition of IPTG to a concentration of 1 mM, incubation was continued for an additional 4.5 h. Cells were harvested by centrifugation at 4000g at 4 °C for 15 min and stored at –80 °C until use. All subsequent operations were performed at 4 °C. The bacterial pellet obtained from 40 mL of culture was resuspended in 1 mL ice-cold TEGDM buffer (10 mM Tris, 1 mM EDTA, 10% glycerol, 10 mM DTT, and 10 mM sodium molybdate). This suspension was subjected to sonication using twelve 7 s bursts on ice (USP-600 A sonicator, Shimadzu, Japan), and crude GST-hARLBD fraction was prepared by centrifugation of the suspension at 12,000g for 30 min at 4 °C. Western blot analysis showed that GST-hARLBD existed in the supernatant cytosolic fraction. This crude receptor fraction was diluted to a protein concentration of 0.3–0.5 mg/mL and used in binding assays as GST-hARLBD fraction. Total protein was determined using a Coomassie Protein Assay Kit. In preliminary experiments, the equilibrium dissociation constant ( $K_d$ ) of testosterone was determined by incubating the GST-hARLBD fraction with increasing concentrations of [<sup>3</sup>H]testosterone (from 0.1 nM to 100 nM final concentration) at 4 °C for 12–18 h. Non-specific binding was assessed by addition of a 1000-fold excess of nonradioactive testosterone. Separation of ligand-bound protein fraction and free radioactive ligand was achieved by Sephadex G-25 gel filtration column chromatography. The protein fraction was collected and the radioactivity was determined with a liquid scintillation counter. Under the experimental conditions, 10 nM [<sup>3</sup>H]testosterone was enough to saturate the binding sites in the GST-hARLBD fraction. All experiments were performed in triplicate or more. To determine the  $K_d$  of [<sup>3</sup>H]testosterone, data were analyzed using a modified form of the Scatchard equation:  $B/F = (-1/K_d) \times B + B_{max}/K_d$ , where  $B$  is the concentration of specifically bound [<sup>3</sup>H]testosterone,  $F$  is the concentration of free [<sup>3</sup>H]testosterone, and  $B_{max}$  is the maximum concentration of available binding sites. Binding competition studies for the test compounds were then performed under identical conditions by incubating increasing concentrations (100 nM–10 μM) of test compound (dissolved in DMSO) with the GST-hARLBD fraction in the presence of a saturating concentration of [<sup>3</sup>H]testosterone (10 nM) at 4 °C for 12–18 h. The concentration of test compounds that inhibited [<sup>3</sup>H]testosterone-binding to the extent of 50% was quantified (IC<sub>50</sub>) after log–logit transformation. The  $K_i$  values were determined by application of the Cheng–Prusoff equation to the IC<sub>50</sub> values, where  $K_i = IC_{50} / \{1 + ([^3H]testosterone)/K_d\}$ .

### 7.15. Measurement of androgen–antagonistic activity by means of SC-3 growth inhibition assay

SC-3 (Shionogi Carcinoma-3) cells were cloned from Shionogi Carcinoma 115 cells, which were established from a mouse breast cancer. SC-3 shows androgen-dependent growth.<sup>32,33</sup> In this assay, androgenic and anti-androgenic activities of test compounds were determined in terms of SC-3 growth promotion and inhibition, respectively. SC-3 cells were cultured in the presence of MEM supplemented with 10% FBS and 10 nM testosterone at 37 °C 5% CO<sub>2</sub>. All experiments were performed in triplicate or more. For SC-3 cell growth-inhibition assay, the cells were trypsinized and diluted to 3.0 × 10<sup>4</sup> cell/mL with MEM supplemented with 10% charcoal resin-stripped fetal bovine serum. This cell suspension was transferred to 96-well microtiter plates, and various concentrations of test compound (from 100 nM to 10 μM DMSO solution) and/or testosterone ethanol solution (final concentration 10 nM) were added. Then the plates were incubated at 37 °C 5% CO<sub>2</sub> for 3 days, and the cell number was determined using the WST-1 method with a Cell Counting Kit and an MPR-A4i2 micro plate reader (TOSOH, Japan). The number of cells on wells with testosterone alone was defined as 100%. The concentration of test compounds that inhibited the increase of the cell number induced by 10 nM testosterone by 50% was quantified (IC<sub>50</sub>) after log–logit transformation. LNCaP growth promotion and inhibition assays were performed by the same method as described for SC-3 assay, except that RPMI1640 medium was used.

### 7.16. General procedure for the preparation of 8–14

To a stirred solution of NaH (2.0 equiv/bisphenol) in DMF (0.3 M) was added bisphenol. The reaction mixture was stirred at 0 °C for 30 min, then 1-chloropinacolone (2.4 equiv) was added and stirring was continued at room temperature for 3 h. The reaction mixture was partitioned between aq NH<sub>4</sub>Cl and ethyl acetate. The organic layer was washed with brine, dried over MgSO<sub>4</sub>, and concentrated. The resulting residue was purified by silica gel chromatography to afford 8–14.

### 7.17. 2,2-Bis[4-(3,3-dimethyl-2-oxobutoxy)-3-methylphenyl]propane (8)

Yield: 79%. White crystals. <sup>1</sup>H NMR (500 MHz, CDCl<sub>3</sub>/δ): 6.99 (s, 2H), 6.93 (dd, *J* = 8.6, 2.6 Hz, 2H), 6.49 (d, *J* = 8.6 Hz, 2H), 4.84 (s, 4H), 2.25 (s, 6H), 1.59 (s, 6H), 1.25 (s, 18H). <sup>13</sup>C NMR (125 MHz, CDCl<sub>3</sub>/δ): 210.0, 154.1, 143.5, 129.6, 126.4, 124.7, 110.4, 69.5, 43.2, 41.5, 31.0, 26.3, 16.6. HRMS (FAB, M+H<sup>+</sup>) calcd for C<sub>29</sub>H<sub>41</sub>O<sub>4</sub>, 453.3005, found 453.3011.

### 7.18. 4,4-Bis[4-(3,3-dimethyl-2-oxobutoxy)-3-methylphenyl]heptane (10)

Yield: 60%. White crystals. <sup>1</sup>H NMR (500 MHz, CDCl<sub>3</sub>/δ): 6.91 (s, 2H), 6.87 (dd, *J* = 8.6, 2.6 Hz, 2H), 6.47 (d, *J* = 8.6 Hz, 2H), 4.83 (s, 4H), 2.24 (s, 6H), 1.94–1.90 (m, 4H), 1.25 (s, 18H), 0.96–0.92 (m, 4H), 0.83

(t, *J* = 7.3 Hz, 6H). <sup>13</sup>C NMR (125 MHz, CDCl<sub>3</sub>/δ): 210.1, 153.9, 142.0, 130.5, 125.9, 125.9, 110.1, 69.6, 48.0, 43.2, 40.3, 26.3, 17.3, 16.7, 14.8. HRMS (FAB, M<sup>+</sup>) calcd for C<sub>33</sub>H<sub>48</sub>O<sub>4</sub>, 508.3553, found 508.3542.

### 7.19. 1,1-Bis[4-(3,3-dimethyl-2-oxobutoxy)-3-methylphenyl]cyclobutane (11)

Yield: 87%. White solid. <sup>1</sup>H NMR (500 MHz, CDCl<sub>3</sub>/δ): 7.05 (s, 2H), 7.00 (dd, *J* = 8.6, 2.7 Hz, 2H), 6.52 (d, *J* = 8.6 Hz, 2H), 4.81 (s, 4H), 2.64 (t, *J* = 7.7 Hz, 4H), 2.26 (s, 6H), 1.91 (quint, *J* = 7.7 Hz, 2H), 1.25 (s, 18H). <sup>13</sup>C NMR (125 MHz, CDCl<sub>3</sub>/δ): 210.0, 154.1, 142.8, 128.9, 126.8, 124.1, 110.8, 69.6, 49.9, 43.2, 35.1, 26.3, 16.6, 16.5. HRMS (FAB, M<sup>+</sup>) calcd for C<sub>30</sub>H<sub>40</sub>O<sub>4</sub>, 464.2927, found 464.2931.

### 7.20. 1,1-Bis[4-(3,3-dimethyl-2-oxobutoxy)-3-methylphenyl]cyclopentane (12)

Yield: 67%. White crystals. <sup>1</sup>H NMR (500 MHz, CDCl<sub>3</sub>/δ): 7.01 (s, 2H), 6.98 (dd, *J* = 8.6, 2.6 Hz, 2H), 6.48 (d, *J* = 8.6 Hz, 2H), 4.81 (s, 4H), 2.24 (s, 6H), 2.22–2.18 (m, 4H), 1.67–1.65 (m, 4H), 1.24 (s, 18H). <sup>13</sup>C NMR (125 MHz, CDCl<sub>3</sub>/δ): 210.0, 154.1, 141.8, 129.8, 126.4, 124.8, 110.5, 69.6, 54.3, 43.2, 38.8, 26.4, 23.0, 16.6. HRMS (FAB, M<sup>+</sup>) calcd for C<sub>31</sub>H<sub>42</sub>O<sub>4</sub>, 478.3083, found 478.3104.

### 7.21. 1,1-Bis[4-(3,3-dimethyl-2-oxobutoxy)-3-methylphenyl]cycloheptane (14)

Yield: 88%. White crystals. <sup>1</sup>H NMR (500 MHz, CDCl<sub>3</sub>/δ): 6.92 (s, 2H), 6.87 (dd, *J* = 8.6, 2.1 Hz, 2H), 6.48 (d, *J* = 8.6 Hz, 2H), 4.82 (s, 4H), 2.23 (s, 6H), 2.22–2.20 (m, 4H), 1.66–1.64 (m, 4H), 1.56–1.54 (m, 4H), 1.25 (s, 18H). <sup>13</sup>C NMR (125 MHz, CDCl<sub>3</sub>/δ): 210.0, 153.9, 143.9, 130.0, 126.3, 125.1, 110.4, 69.6, 48.7, 43.2, 40.5, 30.1, 26.3, 24.3, 16.7. HRMS (FAB, M<sup>+</sup>) calcd for C<sub>33</sub>H<sub>46</sub>O<sub>4</sub>, 506.3396, found 506.3400.

### 7.22. 3,3-Bis[4-(3,3-dimethyl-2-oxobutylamino)-3-methylphenyl]pentane (DPP-1111: 15)

<sup>1</sup>H NMR (500 MHz, CDCl<sub>3</sub>/δ): 6.95 (dd, *J* = 8.5, 2.1 Hz, 2H), 6.85 (d, *J* = 2.1 Hz, 2H), 6.39 (d, *J* = 8.5 Hz, 2H), 4.50 (br, 2H), 4.13 (s, 4H), 2.16 (s, 6H), 1.99 (q, *J* = 7.3 Hz, 4H), 1.24 (s, 18H), 0.59 (t, *J* = 7.3 Hz, 6H). <sup>13</sup>C NMR (125 MHz, CDCl<sub>3</sub>/δ): 211.7, 142.6, 138.0, 130.3, 126.5, 121.6, 109.3, 48.9, 48.2, 43.2, 29.5, 26.6, 17.7, 8.6. HRMS (FAB, M<sup>+</sup>) calcd for C<sub>31</sub>H<sub>46</sub>N<sub>2</sub>O<sub>2</sub>, 478.3559, found 478.3562.

### 7.23. 1-(4-{3-[4-(3,3-Dimethyl-2-oxobutyl)amino-3-methylphenyl]pentan-3-yl}-2-methylphenoxy)-3,3-dimethylbutan-2-one (DPP-0111: 16)

<sup>1</sup>H NMR (500 MHz, CDCl<sub>3</sub>/δ): 6.93–6.89 (m, 3H), 6.83 (s, 1H), 6.49 (d, *J* = 8.1 Hz, 1H), 6.39 (d, *J* = 8.1 Hz, 1H), 4.82 (s, 2H), 4.50 (br, 1H), 4.13 (d, *J* = 4.3 Hz, 2H), 2.23 (s, 3H), 2.16 (s, 3H), 1.99 (q, *J* = 7.3 Hz, 4H), 1.25 (s, 9H), 1.24 (s, 9H), 0.59 (t, *J* = 7.3 Hz, 6H). <sup>13</sup>C NMR (125 MHz, CDCl<sub>3</sub>/δ): 211.7, 210.1,

153.9, 142.6, 141.9, 137.6, 130.8, 130.2, 126.4, 126.1, 125.8, 121.6, 110.1, 109.1, 69.7, 48.8, 48.3, 43.2, 43.1, 29.4, 26.5, 26.4, 17.7, 16.6, 8.5. HRMS (FAB, M<sup>+</sup>) calcd for C<sub>31</sub>H<sub>45</sub>NO<sub>3</sub>, 479.3399, found 479.3392; Anal. Calcd for C, 77.39; H, 9.37; N, 2.80. Found: C, 77.62; H, 9.46; N, 2.92.

### Acknowledgments

The work described in this paper was partially supported by Grants-in-Aid for Scientific Research from The Ministry of Education, Culture, Sports, Science and Technology, Japan, and the Japan Society for the Promotion of Science.

### References and notes

- Bouillon, R.; Okamura, W. H.; Norman, A. W. *Endocr. Rev.* **1995**, *16*, 200.
- Mangelsdorf, D. J.; Thummel, C.; Beato, M.; Herrlich, P.; Schutz, G.; Umesono, K.; Blumberg, B.; Kastner, P.; Mark, M.; Chambon, P.; Evans, R. M. *Cell* **1995**, *83*, 835.
- Björklund, S.; Almouzni, G.; Davidson, I.; Nightingale, K. P. *Cell* **1999**, *96*, 759.
- Boehm, M. F.; Fitzgerald, P.; Zou, A.; Elgort, M. G.; Bischoff, E. D.; Mere, L.; Mais, D. E.; Bissonnette, R. P.; Heyman, R. A.; Nadzan, A. M.; Reichman, M.; Allegretto, E. A. *Chem. Biol.* **1999**, *6*, 265.
- Swann, S. L.; Bergh, J.; Farach-Carson, M. C.; Ocasio, C. A.; Koh, J. T. *J. Am. Chem. Soc.* **2002**, *124*, 13795.
- Bao, B.-Y.; Hu, Y.-C.; Ting, H.-J.; Lee, Y. -F. *Oncogene* **2004**, *23*, 3350.
- Miller, G. J.; Stapleton, G. E.; Ferrara, A. A.; Lucia, M. S.; Pfister, S.; Hedlund, T. E.; Upadhyya, P. *Cancer Res.* **1992**, *52*, 515.
- Zhao, X.-Y.; Ly, L. H.; Peehl, D. M.; Feldman, D. *Endocrinology* **1997**, *138*, 3290.
- Ishizuka, S.; Kurihara, N.; Miura, D.; Takenouchi, K.; Cornish, J.; Cundy, T.; Reddy, S. V.; Roodman, G. D. *J. Steroid Biochem. Mol. Biol.* **2004**, *89–90*, 331.
- Herdick, M.; Steinmeyer, A.; Carlberg, C. *Chem. Biol.* **2000**, *7*, 885–894.
- Kato, Y.; Nakano, Y.; Sano, H.; Tanatani, A.; Kobayashi, H.; Shimazawa, R.; Koshino, H.; Hashimoto, Y.; Nagasawa, K. *Bioorg. Med. Chem. Lett.* **2004**, *14*, 2579.
- Nakano, Y.; Kato, Y.; Imai, K.; Ochiai, E.; Namekawa, J.; Ishizuka, S.; Takenouchi, K.; Tanatani, A.; Hashimoto, Y.; Nagasawa, K. *J. Med. Chem.* **2006**, *49*, 2398.
- Hosoda, S.; Tanatani, A.; Wakabayashi, K.; Nakano, Y.; Miyachi, H.; Nagasawa, K.; Hashimoto, Y. *Bioorg. Med. Chem. Lett.* **2005**, *15*, 4327.
- Schwartz, G. G.; Hulka, B. S. *Anticancer Res.* **1990**, *10*, 1307.
- Hanchette, C. L.; Schwartz, G. G. *Cancer* **1992**, *70*, 2861.
- Bikle, D. D. *Endocr. Rev.* **1992**, *13*, 765.
- Peehl, D. M.; Skowronski, R. J.; Leung, G. K.; Wong, S. T.; Stamey, T. A.; Feldman, D. *Cancer Res.* **1994**, *54*, 805.
- Jones, G.; Strugnell, S. A.; DeLuca, H. F. *Physiol. Rev.* **1998**, *78*, 1193.
- Wolfe, J. P.; Wagaw, S.; Marcoux, J.-F.; Buchwald, S. L. *Acc. Chem. Res.* **1998**, *31*, 805.
- Hartwig, J. F. *Acc. Chem. Res.* **1998**, *31*, 852.
- Wang, Z. Y.; Hay, A. S. *Synthesis* **1989**, 471.
- Ohtani, I.; Kusumi, T.; Kashman, Y.; Kakisawa, H. *J. Am. Chem. Soc.* **1991**, *113*, 4092.
- Fujishima, T.; Konno, K.; Nakagawa, K.; Kurobe, M.; Okano, T.; Takayama, H. *Bioorg. Med. Chem.* **2000**, *8*, 123.
- Imae, Y.; Manaka, A.; Yoshida, N.; Ishimi, Y.; Shinki, T.; Abe, E.; Suda, T.; Konno, K.; Takayama, H.; Yamada, S. *Biochim. Biophys. Acta* **1994**, *1213*, 302.
- Kagechika, H.; Kawachi, E.; Hashimoto, Y.; Himi, T.; Shudo, K. *J. Med. Chem.* **1988**, *31*, 2839.
- Rochel, N.; Wurtz, J. M.; Mitschler, A.; Klaholz, B.; Moras, D. *Mol. Cell* **2000**, *5*, 173.
- Brooks, B. R.; Bruccoleri, R. E.; Olafson, B. D.; States, D. J.; Swaminathan, S.; Karplus, M. *J. Comput. Chem.* **1983**, *4*, 187.
- Takahashi, H.; Ishioka, T.; Koiso, Y.; Sodeoka, M.; Hashimoto, Y. *Biol. Pharm. Bull.* **2000**, *23*, 1387.
- Roehborn, C. G.; Zoppi, S.; Gruber, J. A.; Wilson, C. M.; McPhaul, M. J. *Mol. Cell. Endocrinol.* **1992**, *84*, 1.
- Sawada, T.; Hashimoto, Y.; Li, Y.; Kobayashi, H.; Iwasaki, S. *Biochem. Biophys. Res. Commun.* **1991**, *178*, 558.
- Sawada, T.; Kobayashi, H.; Hashimoto, Y.; Iwasaki, S. *Biochem. Pharmacol.* **1993**, *45*, 1387.
- Kasayama, S.; Saito, H.; Kouhara, H.; Sumitani, S.; Sato, B. *J. Cell. Physiol.* **1993**, *154*, 254.
- Hiraoka, D.; Nakamura, N.; Nishizawa, Y.; Uchida, N.; Noguchi, S.; Matsumoto, K.; Sato, B. *Cancer Res.* **1987**, *47*, 6560.
- Kainuma, M.; Kasuga, J.; Hosoda, S.; Wakabayashi, K.; Tanatani, A.; Nagasawa, K.; Miyachi, H.; Makishima, M.; Hashimoto, Y. *Bioorg. Med. Chem. Lett.* **2006**, *16*, 3213.
- Dahnke, K. R.; Gajewski, R. P.; Jones, C. D.; Linebarger, J. H.; Lu, J.; Ma, T.; Nagpal, S.; Simard, T. P.; Yee, Y. K.; Bunel, E. E.; Stites, R. E. PCT/US03/14539 (WO 03/101978), 2003.
- Bunel, E. E.; Gajewski, R. P.; Jones, C. D.; Lu, J.; Ma, T.; Nagpal, S.; Yee, Y. K. PCT/US2003/035055 (WO 2004/048309), 2004.
- Gajewski, R. P.; Jones, C. D.; Linebarger, J. H.; Lu, J.; Ma, T.; Nagpal, S.; Yee, Y. K. PCT/US2004/035513 (WO 2005/051898), 2005.